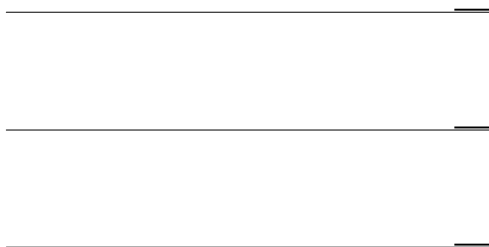


Mineralogical Transformation of a Soil derived from
Volcanic Sediments, Dangsanbong, Jeju Island

Mineralogical Transformation of a Soil derived from
Volcanic Sediments, Dongsanbong, Jeju Island

2001 6



감사의 글

관심과 사랑으로 지도해 주신 문희수 교수님께 깊은 감사를 드립니다. 언제나 건강하시기를 기원합니다. 학부와 대학원 과정 동안 가르침을 주신 민경덕 교수님, 유강민 교수님, 권성택 교수님, 한정상 교수님, 원중선 교수님, 우남철 교수님께 감사를 드립니다.

논문을 처음 시작하던 제주도 필드에서부터 지금까지, 늘 가까이에서 저를 지도해 주시고 가장 큰 힘이 되어주신 두 분께 특별히 감사를 드립니다. 송윤구 교수님, 규호형 고맙습니다.

관심으로 지켜봐 주신 김재곤 박사님과 이수정 박사님께도 감사를 드립니다. 같은 연구실에서 동고동락하던 문지원, 전철민, 성기훈 선배님과 일모, 성윤, 정현, 승신, 용희, 석찬, 신열에게 감사의 마음을 전합니다. 대학원 생활 동안 많은 힘이 되어준 나의 동기들, 원진, 효재, 승찬, 재봉, 형섭을 비롯한 대학원 선후배님들, 그리고 나화련씨께 감사를 드립니다.

힘들 때나 기쁠 때나 함께 해준 종훈, 용준, 준석, 승우, 병민, 재호 이하 FCC 가족들에게 감사의 마음을 전합니다.

지금까지 저를 믿고 지켜봐 준 사랑하는 가족들과 학위의 기쁨을 함께 하고 싶습니다.

.....

.....

.....

1	1
2	3
2.1.	3
2.2.	6
3	8
3.1. pH	8
3.2.	8
3.3.	9
3.4.	9
3.5.	11
3.6. X-	12
3.7. IR	13
4	15
4.1.	15
4.1.1.	15
4.1.2.	, ,	16
4.2.	20
4.2.1. pH,	,	20
4.2.2.	,	22
4.2.3.	23
4.3.	25
4.3.1. XRD	25
4.3.2. IR	36
5	38
5.1. HIS HIV 가?	39
5.2.	42
5.3.	49
5.3.1.	49

5.3.2.	53
6	59
	60
	67

List of Figures

Fig. 1. Geologic map of the Dangsambong volcano and soil profile of sampling site.	4
Fig. 2. Procedures for soil texture analysis.	10
Fig. 3. Procedures for XRD, IR, and Chemical analysis.	14
Fig. 4. Variation in size fractions of bulk samples.	16
Fig. 5. XRD patterns of bulk samples.	18
Fig. 6. XRD patterns of sand size fractions.	19
Fig. 7. XRD patterns of silt size fractions.	19
Fig. 8. Variation of pH with depth.	21
Fig. 9. XRD patterns of clay size fractions, no chemical treatment.	26
Fig. 10. XRD patterns of clay size fractions, after removal of carbonate, organic matter.	29
Fig. 11. XRD patterns of clay size fractions, after removal of carbonate, organic matter and free iron oxide.	32
Fig. 12. XRD patterns of coarse clay size fractions(2-0.2 μm) treated with Na-Oxalate for 4h, after removal carbonate, organic matter, and free iron oxide.	35
Fig. 13. XRD patterns of coarse clay size fractions(2-0.2 μm) saturated with K, after removal of carbonate, organic matter, and free iron oxide, and treated with Na-Oxalate, and Na-citrate for 4h, respectively.	36
Fig. 14. Infrared spectra of C1.	37
Fig. 15. Extractable Al, Fe, and Mg from clay size fractions with DCB, and acid oxalate.	41
Fig. 16. Decomposition for XRD pattern of A1(<0.2 μm), after DCB, and EG treatment.	44
Fig. 17. The proportion of kaolinite in kaolinite/smectite interstratification.	45
Fig. 18. Comparison of XRD patterns.	46
Fig. 19. Decomposition for XRD pattern of A1(0.2-2 μm), after DCB, and EG treatment.	47
Fig. 20. The proportion of chlorite in chlorite/smectite interstratification.	48
Fig. 21. The change of relative amounts of each elements to TiO ₂	50

Fig. 22. Weathering indices of bulk samples.	51
Fig. 23. Trace elements variation diagram for bulk.	52
Fig. 24. Chondrite-normalized Rare Earth Element patterns for bulk.	53
Fig. 25. pH(NaF), Si ₆ and short-range-order materials of bulk samples.	55
Fig. 26. Variation of mineralogical compositions of clay size fractions with depth.	56

List of Tables

Table 1. Mean annual climatic data of Jeju Island.	6
Table 2. Particle size distribution of bulk samples.	15
Table 3. Semiquantitative mineralogical composition of bulk, sand, and silt size fraction based on XRD analysis.	18
Table 4. Properties of the bulk samples.	20
Table 5. Exchangeable cation concentration of the bulk samples.	21
Table 6. Major elements composition of bulk samples.	22
Table 7. Concentrations of trace elements in bulk samples.	23
Table 8. Chondrite-normalized rare earth elements abundances in bulk samples.	23
Table 9. Extractable Al, Si, and Fe from bulk sample by acid oxalate, and Na-pyrophosphate.	24
Table 10. Extracted Si, Al, and Fe by DCB, and acid oxalate from clay size fraction.	24
Table 11. Two theta and d-value for clay size fraction after each chemical treatment and EG treatment.	39
Table 12. The peak position of kaolinite/EG-smectite interstratification.	44
Table 13. Mineral compositions of clay size fraction obtained by NEWMODE.	45
Table 14. The peak position of chlorite/EG-smectite interstratification.	49
Table 15. pH(NaF) and the amounts of short-range-order materials.	54

	Andisols		Andisols	
	A	C	B	
pH(H ₂ O)			(<6.0)	6.6-7.3
가 . pH(NaF)		9.49-9.81		9.4
wt%			2wt% Andisol	0.55-1.02
				Si
	Andisols (22-30wt%)		37-49wt%	
		가 가		
<0.2 μ m				/
		/		
84-86%			가	
		/		가 .
2-0.2 μ m				

, . , .
 / 59-70% 가
 가 . 가 /
 .
 hydroxy-Al/Mg/Fe hydroxy-interlayered vermiculite(HIV)
 hydroxy-interlayered smectite(HIS) . HIV A C
 , hydroxy-Fe/Al . hydroxy-Fe/Al
 가 , HIV
 . HIS C , hydroxy-Mg/Al , hydroxy-Mg가
 .
 가 ,
 HIS , HIV

:
 , , , HIV (hydroxy-interlayered
 vermiculite), HIS (hydroxy-interlayered smectite).

1

4

Andisols

80%

(Shoji *et al.*, 1993).

1,872mm

1.5

2,055mm

1,089mm

Andisols

(Song and

Yoo, 1994; Shin and Tavernier, 1988).

Andisols

(Lee *et al.*, 1983; Song and

Yoo, 1994; Yoo and Song, 1984),

Andisols

(Kim *et al.*, 1986).

pH, CEC,

, XRD

IR

HIV (hydroxy-interlayered vermiculite) HIS (hydroxy-interlayered smectite)가

HIV

(Shin and Tavernier, 1988).

HIV HIS

2

2.1.

1.5km

(Fig. 1a).

(Kim *et al.*, 1986).

가

(Nakamura *et al.*, 1989).

1982).

(, 1976; Lee,

(, 1998).

(spatter)

(lapilli),

(block)

(cinder),

가

(tephra finger jet)

(continuous uprush)

(surtseyan)

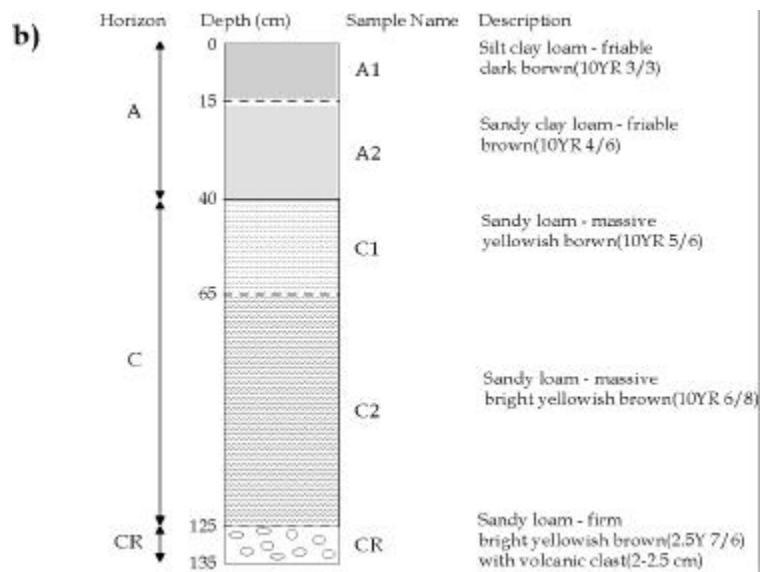
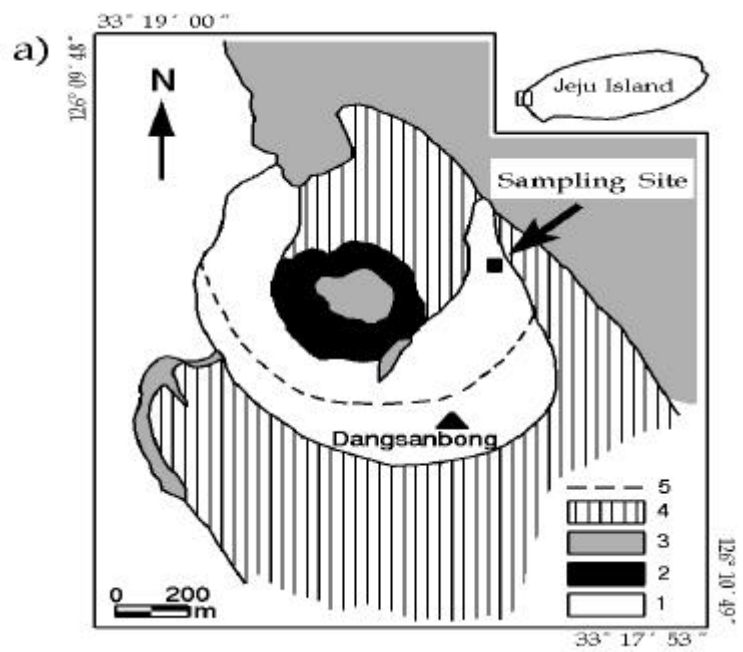


Fig. 1. Geologic map of the Dangsangbong volcano(a) and soil profile of sampling site(b).
1: Dangsangbong tuff cone; 2: cinder cone; 3: basalt lava; 4: Suwolbong tuff; 5: ring fault.

(1998)

1,125m 1,075m (Fig. 1a). 148m

(ash, <2mm), (lapilli, 2-64mm), (block, >64mm), (bed) (shard)

2-5%

vesicular) 35-50% (highly 15-20cm

0.5° (, 1989).

20-40% 가
 400m
 78m
 1m
 20cm

2.2.

1,872mm (, 1992),
 (Table 1). 가
 2,055mm , 가
 1,089mm (, 1999).
 1.5km 1,280mm (1986- 1991)
 (, 1991).

Table 1. Mean annual climatic data of Jeju Island. (1993 ~ 1999)

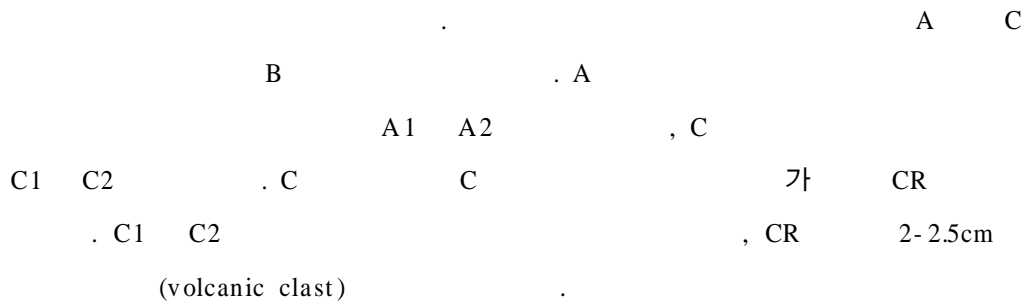
Location	Precipitation (mm)	Evaporation (mm)	Temperature()
East	1,975.6	-	15.2
West	1,089.4	-	15.6
South	2,055.8	1,159.1	16.6
North	1,494.6	1,337.7	16.0
Gosanri	1,280.0	-	-

2.3.

(, 1976).
 30%
 (sandy loam) 가
 (<2wt%)
 (CEC) (13-27me/ 100gr) (base saturation)
 (49-94%).

가

(Fig. 1b).



3

60 , 2mm
2mm
pH, ,
(bulk, <2mm)
XRD IR
(0.2- 2 μ m) (<0.2 μ m)

3.1. pH

pH , 1M KCl, 1M NaF KCl
pH 1:3 1 (Soil
Survey Staff, 1996).

1M NaF pH ,
1:50 (Fieldes and Perrot, 1966).

3.2.

(cation exchange capacity, CEC) 1M NH₄OAc(pH 7)
(Soil Survey Staff, 1992). 가

NH_4^+ 가 NH_4^+ boric
 acid(H_3BO_3) . NH_4^+ H_2SO_4
 .
 (base saturation, BS)
 CEC .

3.3.

potassium dichromate($\text{K}_2\text{Cr}_2\text{O}_7$)
 diphenylamine 0.2N Ammonium iron() sulfate hexahydrate
 . (potassium dichromate) 가 200
 가 (hot plate) , 가 5
 가 . diphenylamine 가 0.2N Ammonium iron()
 sulfate hexahydrate .

3.4.

(texture) ,
 (Gee *et al.*, 1998). wet sieving
 (Fig. 2)
 10g NaOAc(pH 5) 40ml
 . (shaker) 24
 가 .
 (hydrogen peroxide, H_2O_2) ,
 NaOAc(pH 5) (buffer) . 10g (bulk)
 10ml H_2O_2 20ml NaOAc 가 . 90 가
 H_2O_2 .

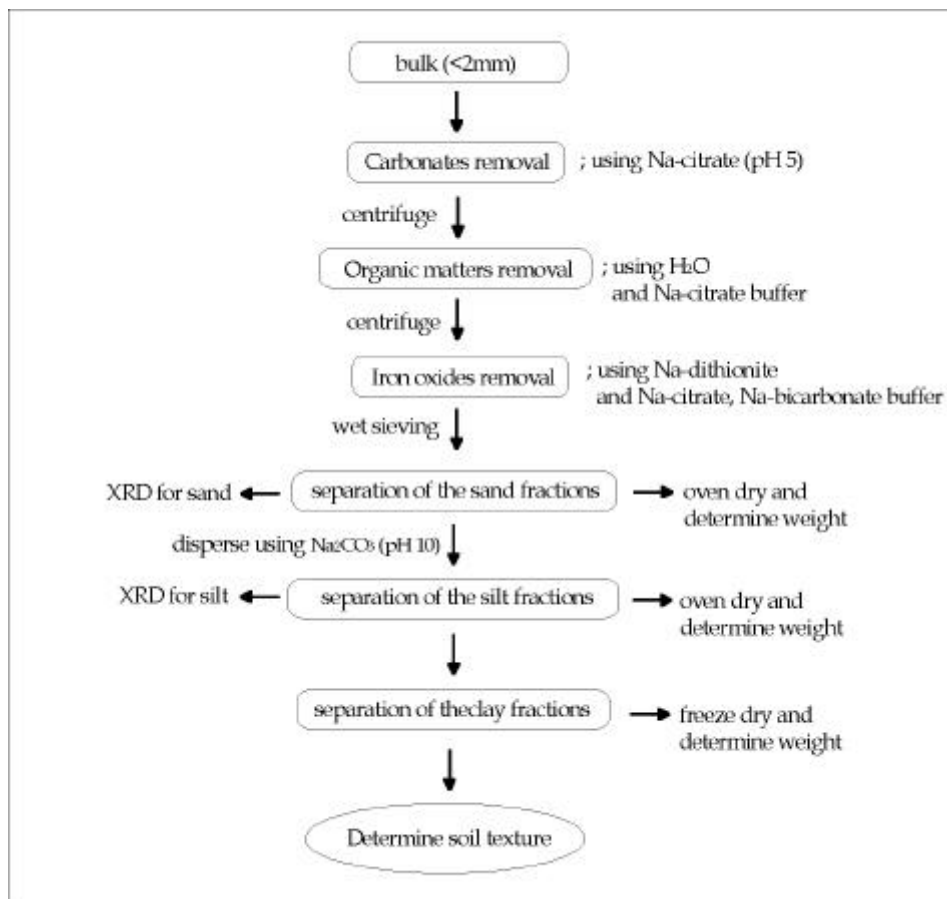


Fig. 2. Procedures for soil texture analysis.

sodium dithionite ($\text{Na}_2\text{S}_2\text{O}_4$), Na-citrate
 Na-bicarbonate (buffer) (DCB).
 10g 0.3M Na-citrate 1M Na-bicarbonate (pH 3) 200ml
 가 . 75 가
 5g Na-dithionite 가 . 1 ,
 15 가 . 10ml NaCl 가
 . 2 .
 ,
 . (sand, $50\mu\text{m}$ -2mm), (silt, 2- $50\mu\text{m}$), (clay, $<2\mu\text{m}$)
 (Jackson, 1985). 0.2- $2\mu\text{m}$ $<0.2\mu\text{m}$.
 46 μm wet sieving .
 . Na_2CO_3 (pH 10) .
 . $<0.2\mu\text{m}$ 0.2-2
 μm .

3.5.

, (rare earth element, REE)
 ,
 .
 , REE
 Royal Holloway and Bedford New College ICP-AES
 (Inductively Coupled Plasma Emission Spectrometry)
 (Walsh, 1980).

Na-pyrophosphate acid oxalate
 (McKeague and Day, 1966). Si, Al, Fe

ICP-AES

1g Na-pyrophosphate(pH 10) 100ml 가 12
3000rpm 30 . Acid oxalate
NH₄-oxalate . 300mg 0.15M (pH 3) 150ml
가 4 .
3000rpm 30 .

3.6. X-

X- (XRD) , , 가 MXP
18A RINT-2500 X- (MacScience Co., Ltd, Japan) .
CuK , 40kV/30mA, 1mm, 1mm, 0.15mm
XRD <2mm

(Fig. 3).

0.2-2 μ m <0.2 μ m XRD

(filter transfer method)

(Moore and Reynolds, 1989).

KCl, MgCl₂ 1N .

(desiccator)

. K 110 , 300 , 550

, 2 . Mg

ethylene glycol(EG) . EG

XRD .

(Fig. 3).

, DCB , acid oxalate
NaOAc(pH 5)

XRD

DCB (<2 μ m) 0.3M
Na-citrate 1M Na-bicarbonate (pH 3) 가 7
5 가 0.5g Na-dithionite 가 15
3000rpm 30 2

DCB NH₄-oxalate , DCB 2
0.15M NH₄-oxalate(pH 3) 가 4
XRD 0.2- 2 μ m

<0.2 μ m
DCB, NH₄-oxalate, Na-citrate , DCB
NH₄-oxalate 0.3M Na-citrate 가 100
4 DCB
XRD 0.2- 2 μ m <0.2 μ m

3.7. IR

FT-IR

(Fig. 3).

XRD

, K

300 , 550

KBr 1:250

(10

0) . IR 가 ,
 (resolution) 2cm^{-1} (interval) 1cm^{-1} .

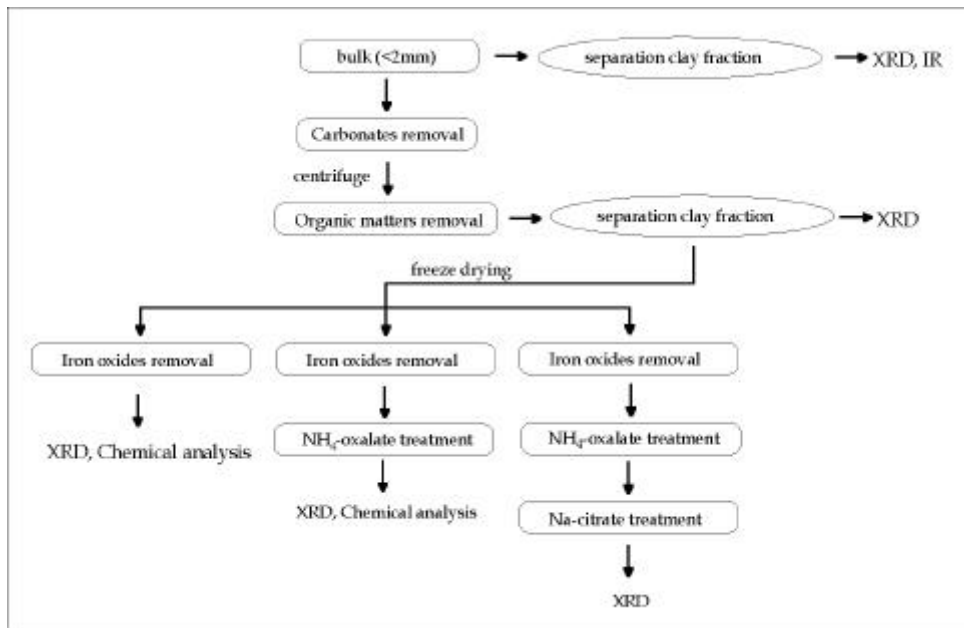


Fig. 3. Procedures for XRD, IR, and Chemical analysis.

4

XRD

4.1.

4.1.1.

Table 2 (bulk, <2mm) .
 가 가 가 , (Fig.
 4). A1 49wt% 가 33wt%,
 18wt% , . A2 49wt% A1
 2.5 , 26wt% .
 C1, C2, CR 가
 <0.2 μ m 0.2-2 μ m ,
 가 .

Table 2. Particle size distribution(wt%) of bulk samples.

sample	sand 50 μ m- 2mm	silt 2- 50 μ m	clay			soil texture
			total <2 μ m	coarse 0.2- 2 μ m	fine <0.2 μ m	
A1	17.85	49.12	33.01	12.42	20.59	silt clay loam
A2	49.11	26.74	24.14	8.56	15.58	sandy clay loam
C1	61.99	19.55	18.44	6.12	12.30	sandy loam
C2	66.80	18.70	14.48	4.83	9.64	sandy loam
CR	75.27	17.79	6.93	2.80	4.12	sandy loam

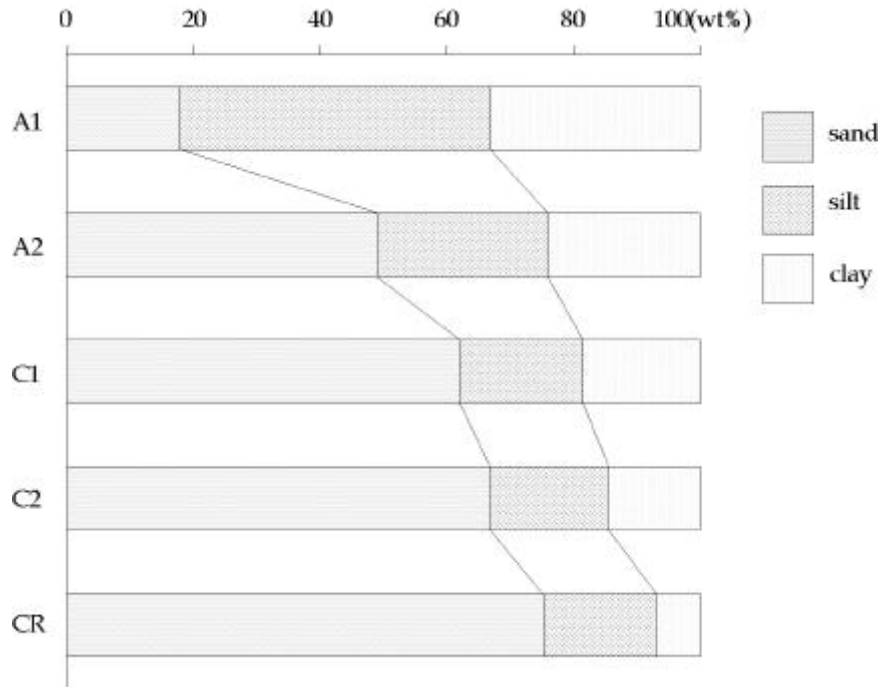


Fig. 4. Variation in size fractions of bulk samples.

4.1.2. , ,

, , (Fig. 5, 6, 7).

XRD

(Table 3).

A1 , , . , ,
 .
 (NaAlSi₃O₈ - CaAl₂Si₂O₈) K-

(KAlSi₃O₈)

K-

. K-

A2

C1

C2

. C2

CR

가

C1 A

, C1 A

A
CR

CR

, K-

A

K-

, K-

C2

. CR

. C1 A

Table 3. Semiquantitative mineralogical composition of bulk, sand, and silt size fraction based on XRD analysis.

	31			32			33		
	bulk	sand	silt	bulk	sand	silt	bulk	sand	silt
Qz	++++	++++	++++	+++	+	+++	++	+	+++
Ol	+	++	+	(-)	+	nd	+	+++	nd
Pl	++	+	++	+	nd	++	(-)	nd	++
Fd	K	+	+	nd	(-)	nd	+	nd	nd

	34			35		
	bulk	sand	silt	bulk	sand	silt
Qz	+	(-)	++	nd	nd	nd
Ol	++++	+++	++	++++	++++	+
Pl	nd	nd	nd	+++	+++	++++
Fd	K	nd	nd	nd	nd	nd

Qz: Quartz; Ol: Olivine; Fd: Feldspar; Pl: Plagioclase series; K: K-feldspar series; +: the number is relative amounts of each mineral; (-): negligible; nd: not detected.

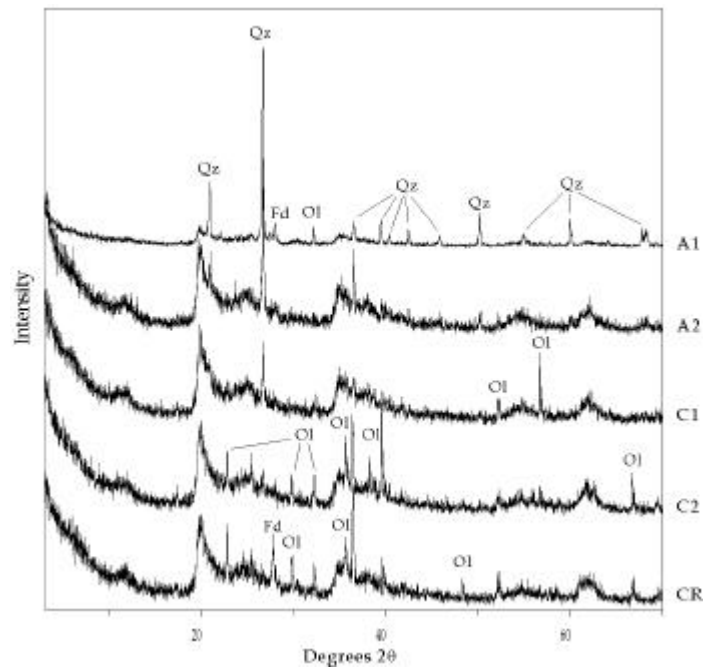


Fig. 5. XRD patterns of bulk samples. Qz: quartz; Ol: olivine; Fd: feldspar.

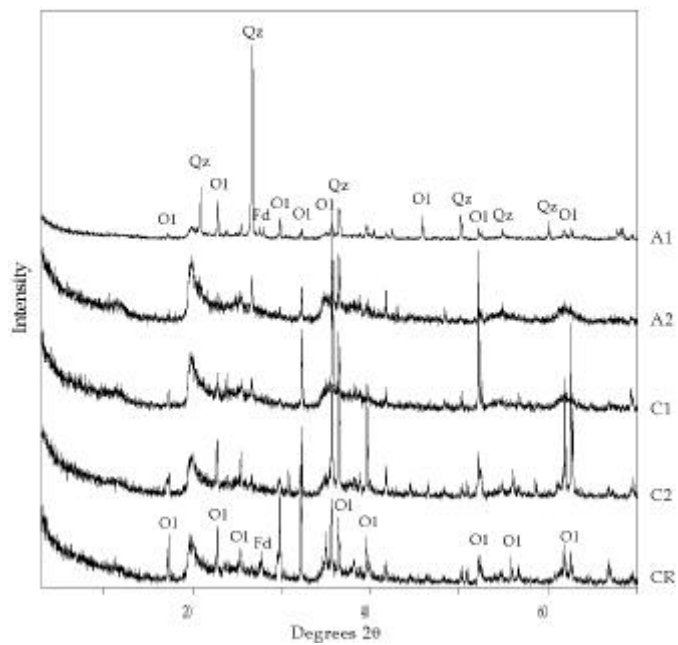


Fig. 6. XRD patterns of sand size fractions. Qz: quartz; Ol: olivine; Fd: feldspar.

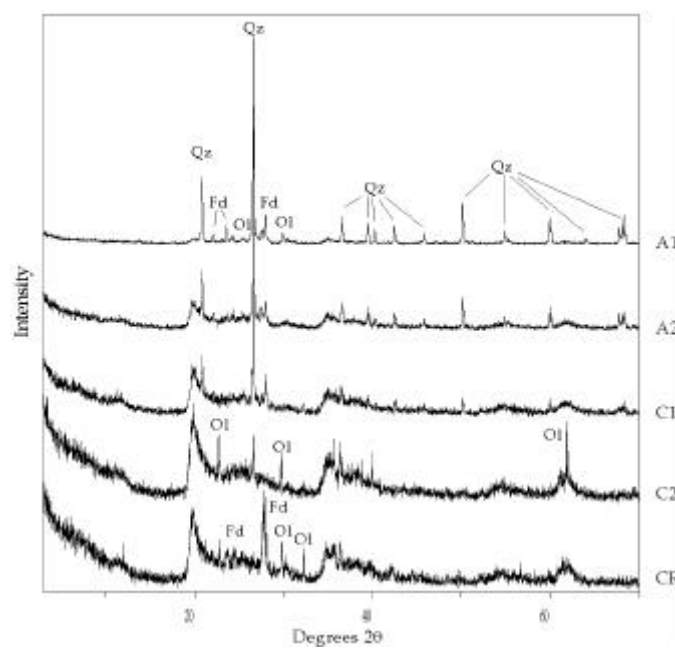


Fig. 7. XRD patterns of silt size fractions. Qz: quartz; Ol: olivine; Fd: feldspar.

4.2.

4.2.1. pH, ,

pH(H₂O) 6.6-7.3 , A1 가
 가 C (Table 4.). pH(KCl) 5.1-5.3
 , 가 (Fig. 8). pH(NaF) 9.5-9.8 ,
 가 . pH(NaF)
 9.4
 (Fieldes and Perrott, 1966).

(cation exchange capacity, CEC) 19-35cmol/kg 가
 C1 C2 . CR 30cmol/kg A
 (A1, A2) .
 A1 A2 2-1.2wt% , 1wt%

Table 4. Properties of the bulk samples.

Sample	Depth (cm)	pH			CEC (cmol./kg)	BS (%)	O.C (wt%)
		H ₂ O(1:3)	KCl(1:3)	NaF(1:50)			
A1	0- 15	6.632	5.338	9.49	19	75.32	2.00
A2	15- 40	7.073	5.213	9.63	26	125.69	1.21
C1	40- 65	7.197	5.162	9.53	35	109.76	0.59
C2	65- 125	7.257	5.364	9.55	32	127.07	0.84
CR	125- 135	7.375	5.303	9.81	30	126.59	0.80

O.C: Organic contents; CEC: Cation exchange capacity; BS: Base saturation,

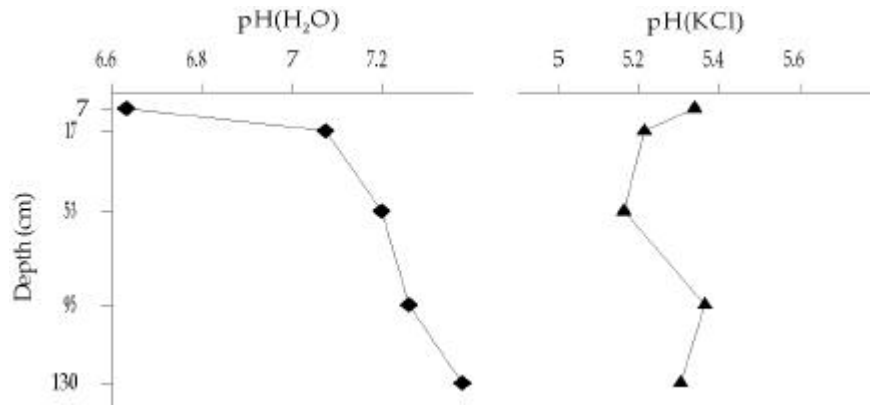


Fig. 8. Variation of pH with depth.

(base saturation, BS) A1 75.32%
 100% Ca²⁺ Mg²⁺가
 K⁺ Na⁺ (Table 5).
 A1 가 (14cmol/kg)
 (32-40cmol/kg). Mg²⁺ C, Ca²⁺ C2 CR
 CEC
 A (A1, A2) 가 C (C1, C2, CR)

Table 5. Exchangeable cation concentration of the bulk samples.

sample	exchangeable cation(cmol/kg)				
	Ca ²⁺	Mg ²⁺	K ⁺	Na ⁺	total
A1	4.47	9.48	0.10	0.33	14.38
A2	9.26	21.59	0.24	1.23	32.32
C1	11.23	25.25	0.23	1.48	38.19
C2	13.51	25.30	0.40	1.46	40.67
CR	13.88	22.20	0.49	1.40	37.97

4.2.2. ,

(bulk, <2mm) Table 6 . SiO₂
 36.4-49.0wt% . SiO₂
 Al₂O₃ 14.1-17.8wt% 가 . Al₂O₃ A1
 14.1wt% A2-C1 17.8wt% . A2-CR 가
 . Fe₂O₃ 11.4-16.5wt%
 A1 A2-CR . MgO CaO 2.0-10.6wt%
 0.15-1.16wt% 가 , 가
 가 .
 Ba, Cr, Ni, V A1
 (Table 7). Co, Cu, Li, Sc, Y
 , . V
 가 가 .
 Li, V, Y, Zn . 가 Li, V ,
 Y, Zn 가 .
 (Taylor and
 McLennan, 1985) (Table 8). (La, Ce,
 Nd)가 (Dy, Yb) .

Table 6. Major elements composition(wt%) of bulk samples.

	SiO ₂	Al ₂ O ₃	Fe ₂ O ₃	MgO	CaO	Na ₂ O	K ₂ O	TiO ₂	P ₂ O ₅	MnO	Total
A1	49.06	14.18	11.43	2.06	0.15	0.60	1.02	1.85	0.08	0.18	82.14
A2	36.88	17.81	16.18	3.26	0.46	0.19	0.38	2.59	0.07	0.21	78.03
C1	36.65	17.81	16.53	5.85	0.51	0.13	0.24	2.66	0.07	0.22	80.82
C2	36.42	15.65	15.60	9.58	0.63	0.08	0.14	2.43	0.07	0.22	80.82
CR	37.59	14.73	14.63	10.63	1.16	0.18	0.09	2.30	0.12	0.21	81.64

Table 7. Concentrations of trace elements in bulk samples.

	Ba	Co	Cr	Cu	Li	Ni	Sc	Sr	V	Y	Zn
ppm											
A1	363	51	351	43	28	284	20	87	141	30	74
A2	460	70	482	61	16	431	29	73	199	17	88
C1	511	74	501	65	18	486	30	73	131	18	100
C2	554	71	474	61	13	493	28	85	109	24	115
CR	481	66	447	60	10	426	27	123	71	32	118

Table 8. Chondrite-normalized of rare earth elements abundance in bulk samples.

	La	Ce	Nd	Sm	Eu	Dy	Yb
A1	134	77	68	44.5	29.1	15.2	10.9
A2	84	84	47	44.6	26.3	12.1	10.1
C1	87	104	44	39.1	29.6	12.6	10.5
C2	109	96	48	39.8	32.4	14.4	11.3
CR	134	86	52	38.5	36.4	17.1	11.7

4.2.3.

acid oxalate Na-pyrophosphate

(Table 9).

Acid oxalate Si 86-244mmol/kg 가
 . Al 154-172mmol/kg A1 가 ,
 A2-CR . Fe
 .
 Na-pyrophosphate Si 31-50mmol/kg 가
 . Al 7-26(mmol/kg) . Fe 9-17mmol /kg
 Si, Al .

Table 9. Extractable Al, Si, and Fe(mmol/kg) from bulk sample by acid oxalate, and Na-pyrophosphate.

	Al _o *	Si _o *	Fe _o *	Al _p **	Si _p **	Fe _p **
A1	172	86	414	26	31	17
A2	152	114	422	19	36	14
C1	151	174	391	12	37	10
C2	152	210	388	8	39	9
CR	154	244	284	7	50	9

* : acid oxalate extractable Al, Si, Fe.

** : Na-pyrophosphate extractable Al, Si, Fe.

DCB acid oxalate
(Table 10.)

DCB Si A1 99mmol/kg 가
가 , C2 가 (Table 10). Al Fe A1
가 , 가 . Mg Al,
Fe (9-20mmol/kg) .

Table 10. Extracted Si, Al, and Fe(mmol/kg) by DCB, and acid oxalate from clay size fraction.

	DCB					Acid oxalate				
	Si	Al	Fe	Mg	Mn	Si	Al	Fe	Mg	Mn
A1	99	213	1379	9	16	96	202	104	16	nd
A2	129	141	1186	10	12	118	171	118	30	nd
C1	147	87	872	20	10	183	169	166	108	1
C2	161	84	750	16	7	158	158	163	62	nd
CR	135	89	516	14	9	197	253	238	39	2

nd: not detected.

Acid oxalate Mg XRD C1
 C2 62-108mmol/kg A1, A2 . Fe C1 C2
 , Si 96-197mmol/kg 가 가 .
 A1 A2, C1, C2 A1 CR .

4.3.

XRD IR
 0.2- 2 μ m < 0.2 μ m

4.3.1. XRD

XRD
 , XRD
 DCB,
 acid oxalate, Na-citrate .
 ;
 XRD . 0.2-2 μ m XRD 14.24 , 12.0
 , 10.04 , 7.14 (Fig. 9A). 14.24 A1-C2
 , CR (broad) . 10.04 A1-C2
 CR . 12 A1, A2
 C1 . 7.14 A1-C2 . 3.34
 . 3.34 A1-C2 , CR
 (intensity)가 . CR 3.22 .

<0.2 μm 14.10 , 10.04 , 7.40 가 (Fig. 9B). 14.10 A1-CR ,

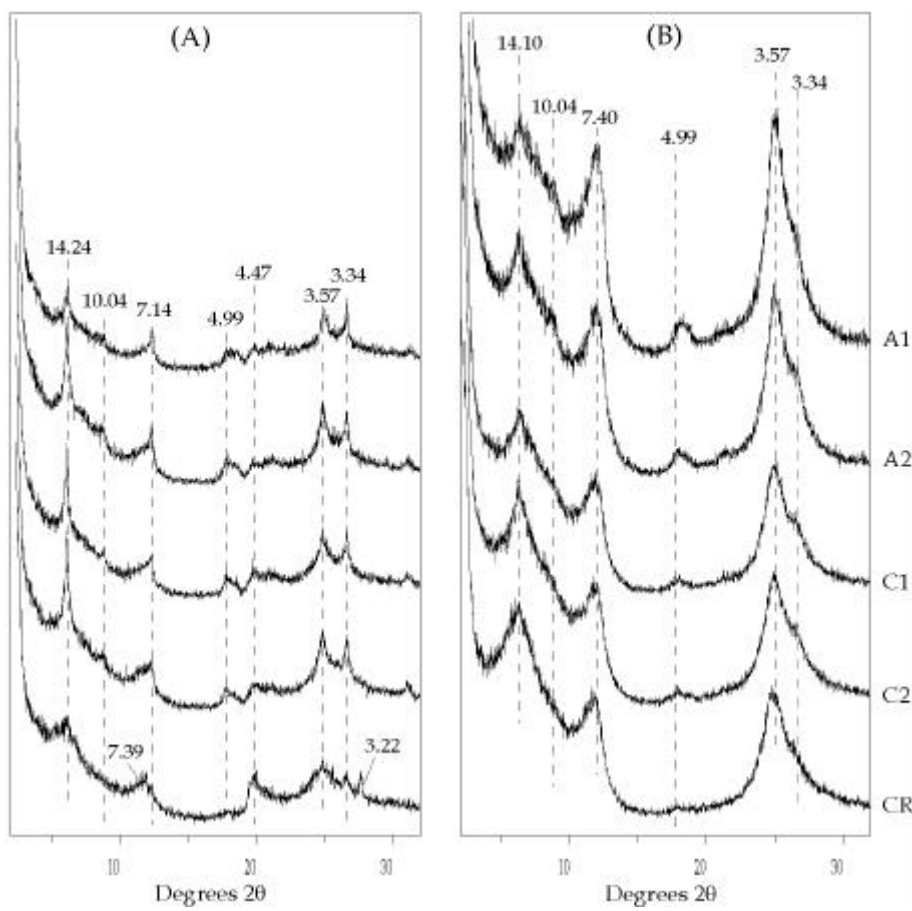


Fig. 9. XRD patterns of untreated clay size fractions. A: 0.2-2 μm ; B: <0.2 μm

K Mg

XRD . K 300 , 550
, Mg (EG)

Fig. 10 .

A1 0.2-2 μ m K XRD 14 , 12
, 10.0 , 7.13 . 300 14

HIS (hydroxy - interlayered smectite) HIV (hydroxy - interlayered
vermiculite) . 550 300 14 가
, 12 . 14
. 12 가 , 550
가 . 550

K 7.13 가 .
가 . Mg 14.10

, 12.00 , 10.04 , 7.13 . 14.10 EG
, 10.04 . EG 14

7.13 (shoulder)
가 (Brindley, 1966; Suquet *et al.*, 1975).

A1 <0.2 μ m K 10.04 , 7.36 .
10.04 Mg 14.10 10
. 10 4.99 . 14

EG 가
. 7.36 550 , Mg

EG .
가 .

A2 0.2-2 μ m K , , Mg , EG A1

. K 14.10 HIV, HIS , 12.00
 가 . 12.00 550
 . A2 550 가 . A2
 , , 2:1 .
 HIV, HIS 가 .
 A2 <0.2 μ m K , , Mg , EG A1
 .
 C1 C2 0.2-2 μ m K , , Mg , EG
 A1, A2 . K
 12 가 , 550 가 12 가 . EG
 A1, A2 가 , 14.10
 A1, A2 . 2:1
 , 12 .
 C1 C2 <0.2 μ m K , , Mg , EG
 2:1 . EG 7.6
 A1 가 가 , 18
 가 .
 CR 0.2-2 μ m XRD . K
 10 7
 . CR <0.2 μ m 10 , 7.5
 . 10 Mg 14 , EG
 , 7.5 EG .
 가 . 4.99 ,
 가 .
 CR <0.2 μ m <0.2 μ m . 18
 .

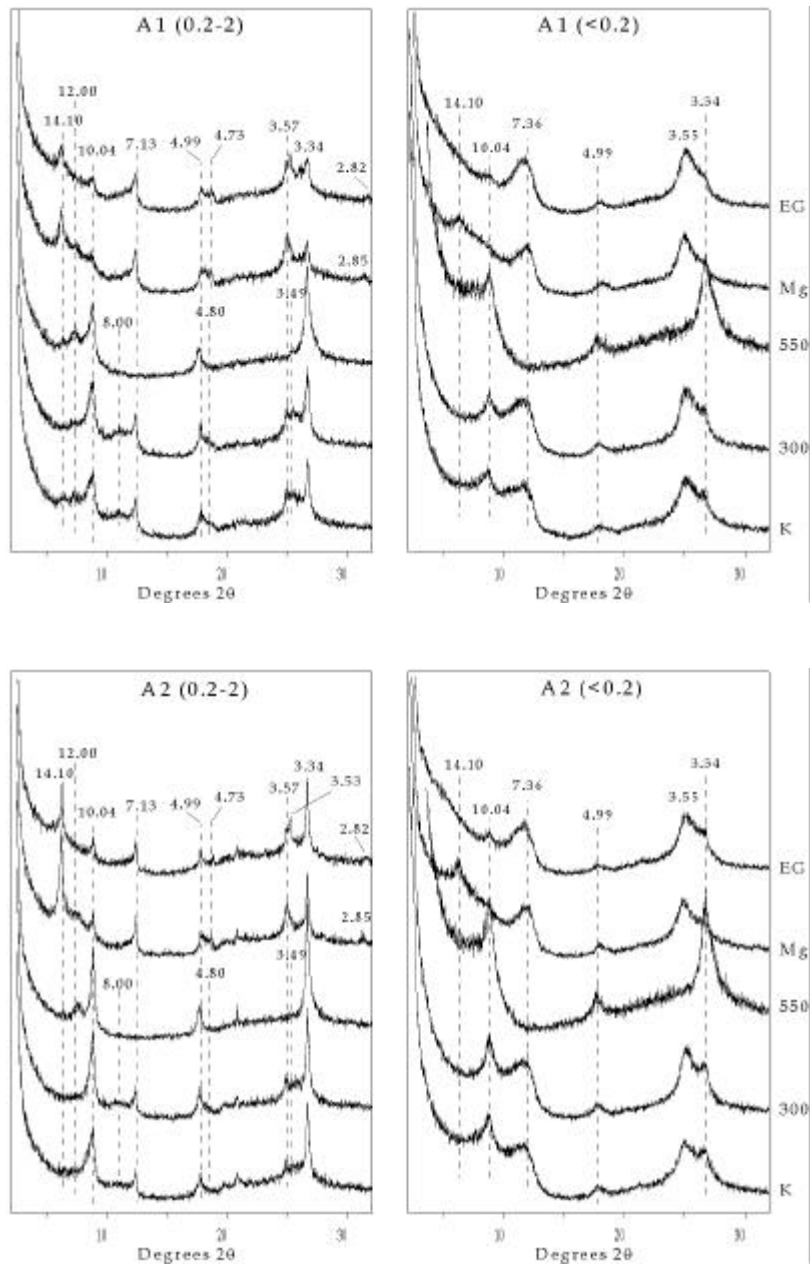


Fig. 10. XRD patterns of clay size fractions, after removal of carbonate, organic matter.
 K: K saturated; 300, 550: heated at 300 °C, and 550 °C for 2 hours after K saturation;
 Mg: Mg saturated; EG: Etylene glycol treated after Mg saturation.

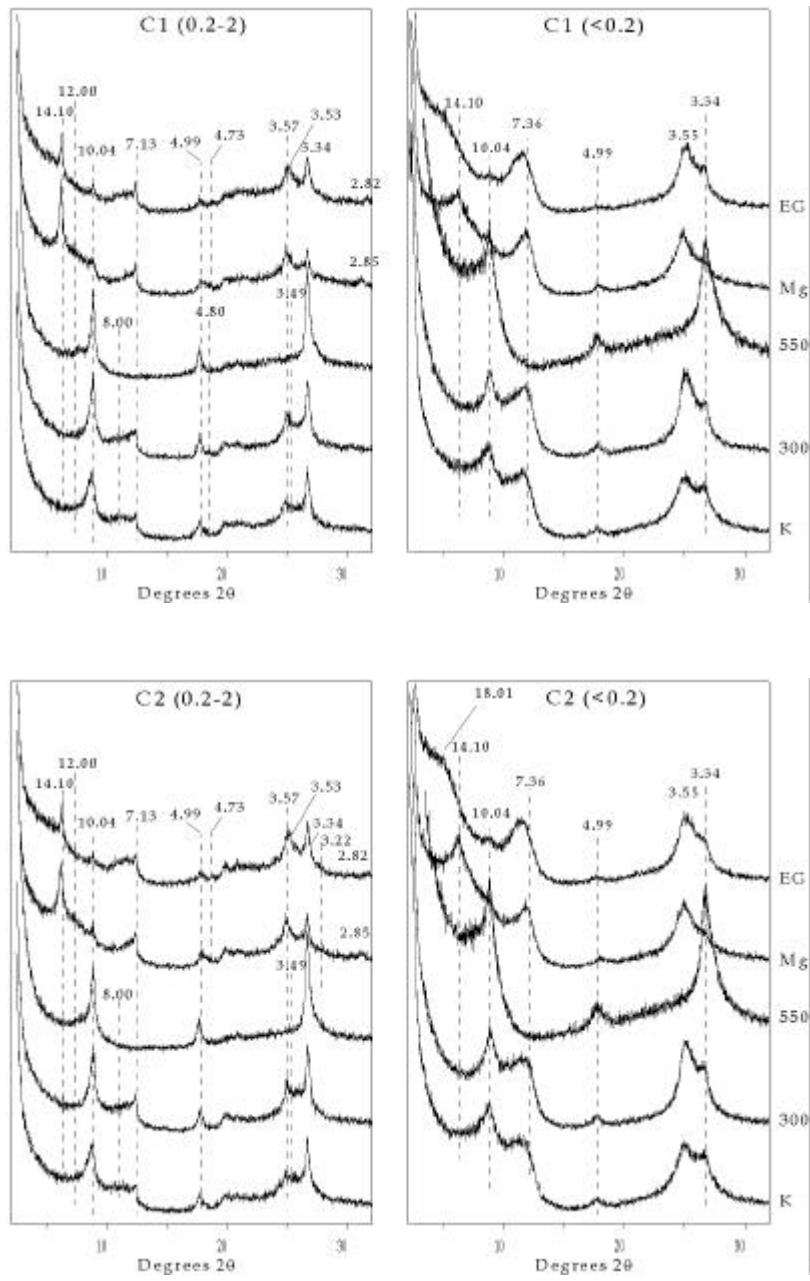


Fig. 10. continued.

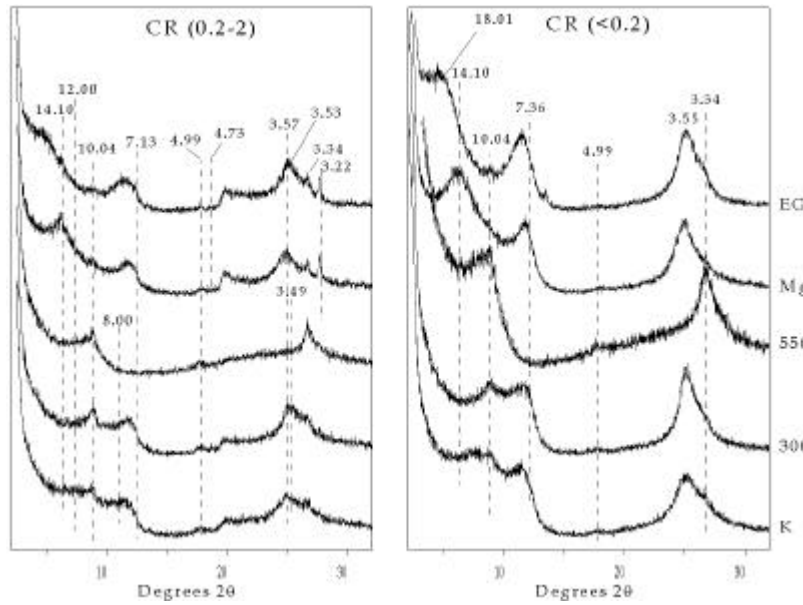


Fig. 10. continued.

		XRD ;			
		DCB, acid oxalate	Na-citrate		
A1	0.2-2 μ m	K	14	DCB	
		, acid oxalate	(Fig. 11,12)	HIV	HIS
		hydroxy-interlayered Al/Mg/Fe	(hydroxy-Al/Mg/Fe)가		
		. EG	2:1		
		HIV . A1 acid oxalate	550		
			14		
			K	3.52	3.57
		(004)	(002)		
A2	0.2-2 μ m	DCB, acid oxalate	EG		16
가	(Fig. 11,12).	DCB			
DCB	HIV	HIS		hydroxy-Al/Mg/Fe가	

가
 C1 C2 0.2-2 μ m XRD
 . EG DCB , DCB
 16 , acid oxalate
 (Fig. 11,12). HIV HIS hydroxy-Al/Mg/Fe
 가 DCB, acid oxalate

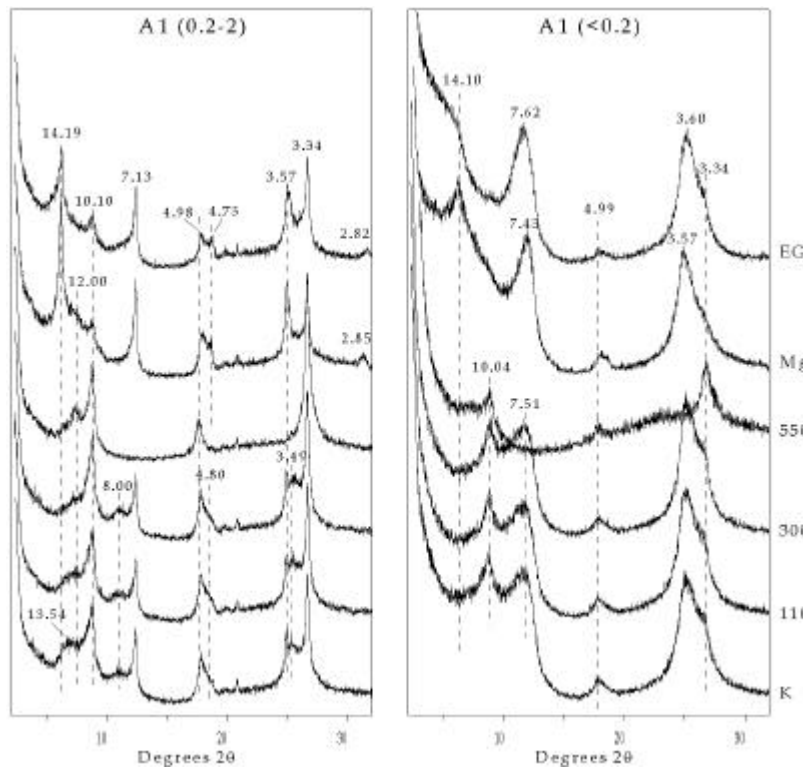


Fig. 11. XRD patterns of clay size fractions, after removal of carbonate, organic matter and free iron oxide. K: K saturated; 110, 300, 550: heated at 110 , 300 , and 550 for 2 hours after K saturation; Mg: Mg saturated; EG: Etylene glycol treated after Mg saturation.

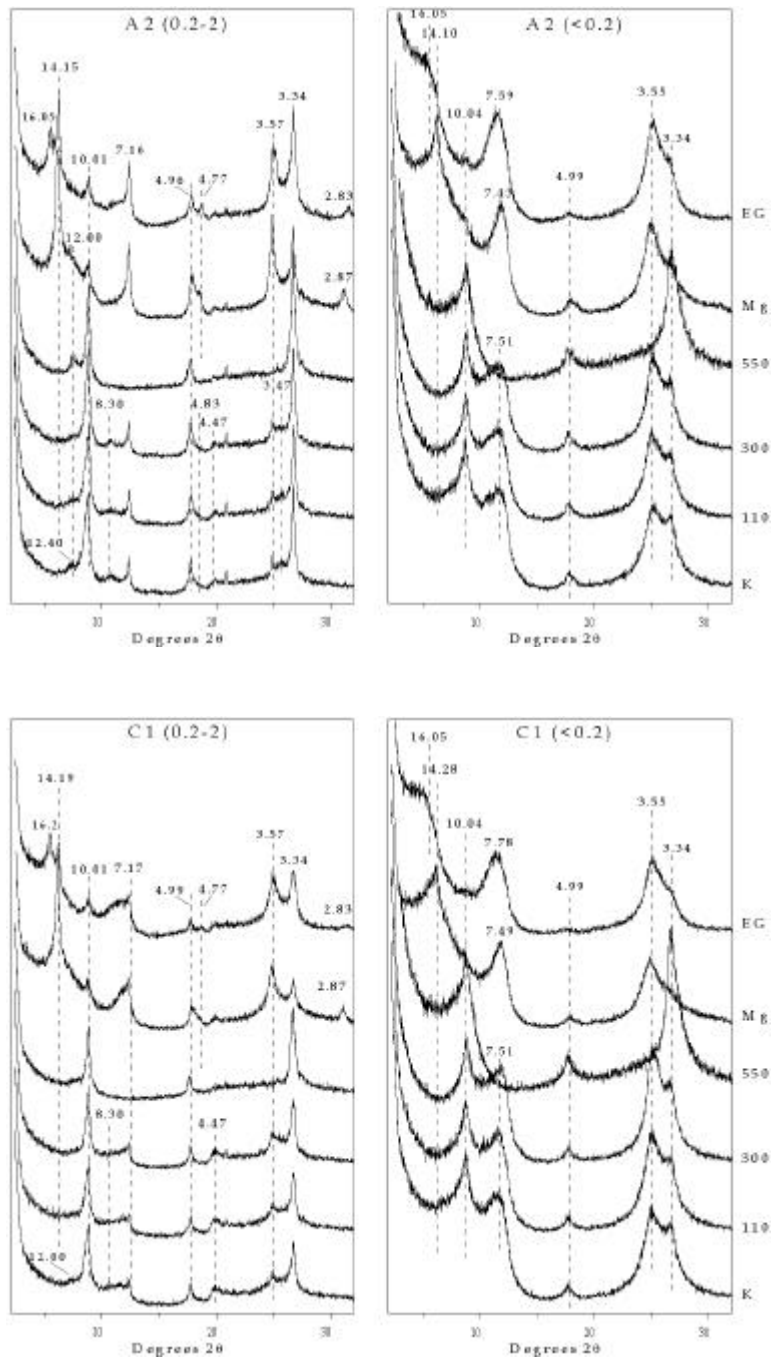


Fig. 11. continued.

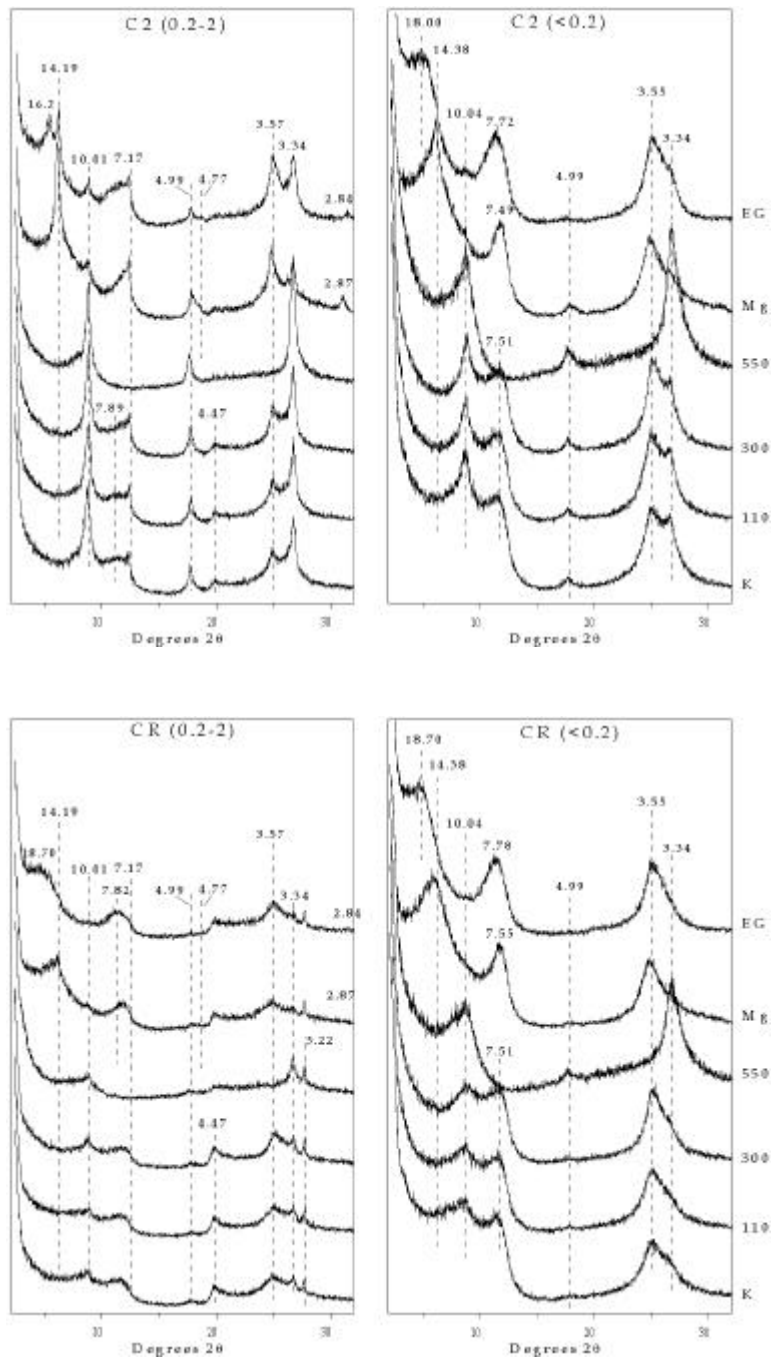


Fig. 11. continued.

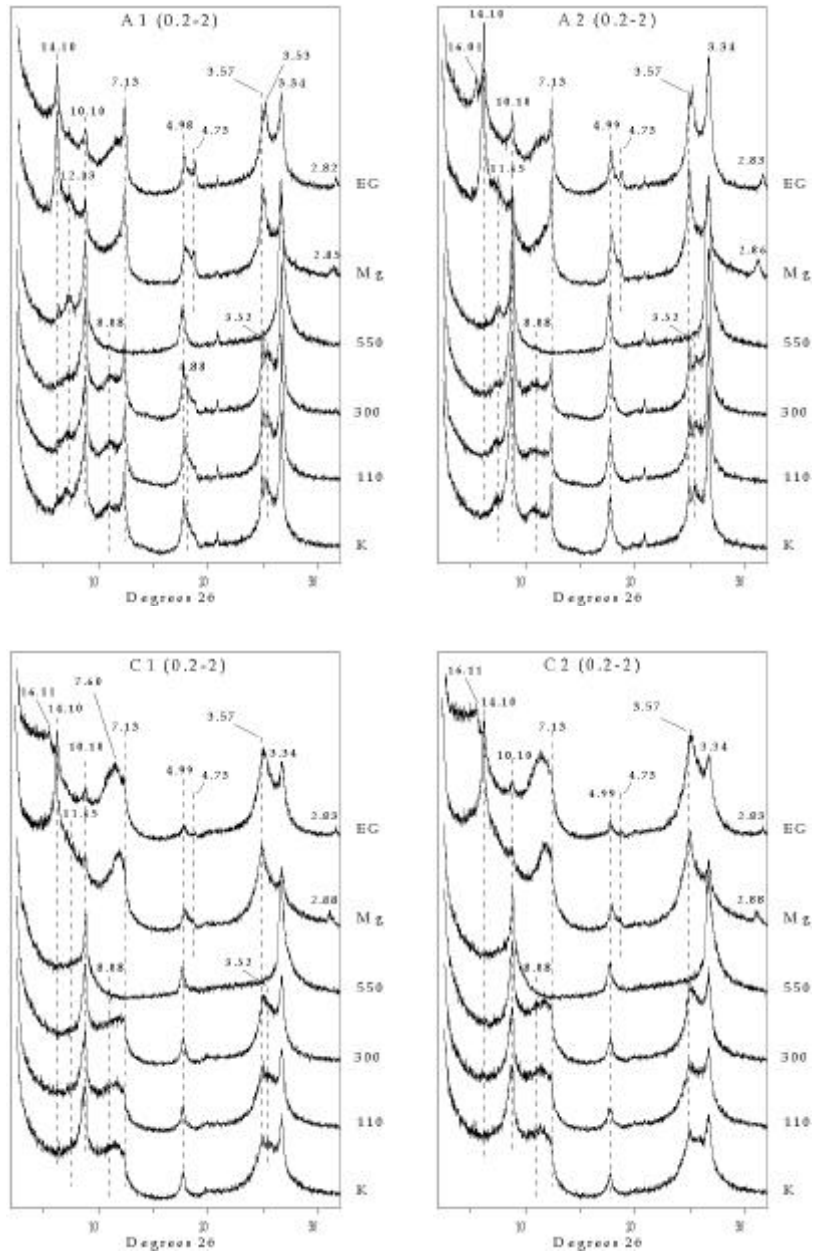


Fig. 12. XRD patterns of coarse clay size fractions(2-0.2 μ m) treated with Na-Oxalate for 4h, after removal carbonate, organic matter, and free iron oxide. K: K saturated; 110, 300, 550: heated at 110 , 300 , and 550 for 2 hours after K saturation; Mg: Mg saturated; EG: Etylene glycol treated after Mg saturation.

DCB acid oxalate Na-citrate
 K XRD (Fig. 13).
 K A1 A2
 12 8 가 HIV HIS 가

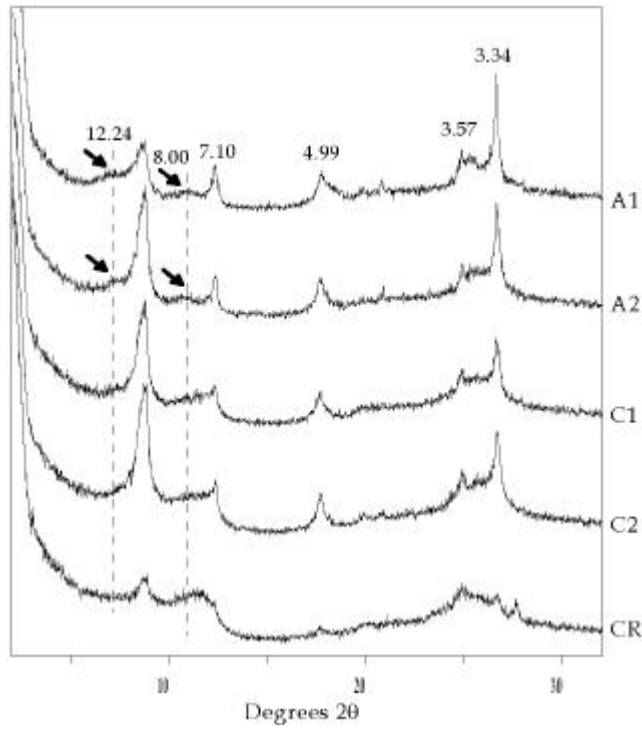


Fig. 13. XRD patterns of coarse clay size fractions(2-0.2 μ m) saturated with K, after removal of carbonate, organic matter, and free iron oxide, and treated with Na-Oxalate, and Na-citrate for 4h, respectively.

4.3.2. IR

Fig. 14 C1 FT-IR
 C1 OH

3750-3400cm⁻¹ 3700, 3620cm⁻¹ 가
 550
 0.2-2μm 880cm⁻¹
 , DCB

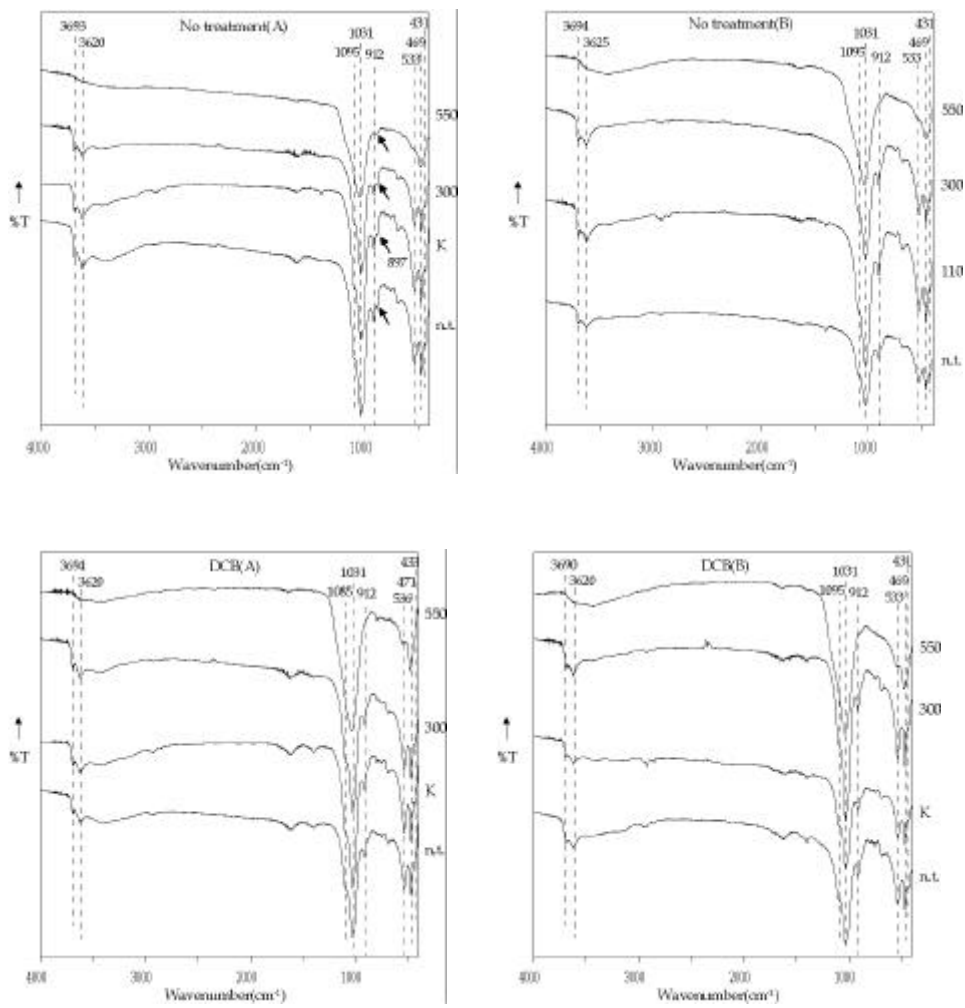


Fig. 14. Infrared spectra of C1. Upper one is untreated and lower one is treated with DCB. A: 2-0.2μm; B: <0.2μm.

5

XRD , , A
 , A CR C
 XRD .
 , , 2:1
 , 1:1 . 0.2-2 μ m XRD
 , 2:1 ,
 1:1 .
 가
 (002) (004)
 (, 1996), Acid oxalate 가
 A
 (001) (004) 가 Fe
 . C acid oxalate EG
 14 .
 CR 0.2-2 μ m , . <0.2 μ m
 CR 0.2-2 μ m .
 HIV, HIS
 (Zhang *et al.* 1994; Bautista-Tulin, 1997;
 Inoue, 1981; Mizota, 1982). XRD
 HIV, HIS 가 .
 HIV, HIS ,

5.1. HIV HIS 가?

0.2-2 μ m Mg EG 가
 (Table 11). XRD HIV HIS 가
 HIV HIS
 (hydroxy-interlayered material)
 hydroxy-Al hydroxy-Mg가 , hydroxy-Fe가
 (Quigley and Martin, 1963; Thomas and Coleman, 1964; Singleton and
 Harward, 1971). HIV hydroxy-Al/Mg/Fe EG
 (Bautista-Tulin, 1997; Inoue, 1981). HIV HIS
 hydroxy-Al/Mg/Fe acid oxalate DCB
 (Rich, 1986; Wada and Kakuto, 1983; Matsue and Wada, 1988; Barnhisel
 and Berstch, 1989; Ghabru, 1990). Hydroxy-Al/Mg/Fe가
 EG HIV HIS
 가

Table 11. Two theta and d-value for clay size fraction(0.2-2 μ m) after each chemical treatment and EG treatment.

	Carbonate, and OM*		DCB		Acid oxalate	
	2 θ	d(Å)	2 θ	d(Å)	2 θ	d(Å)
A1	6.26	14.10	6.22	14.19	6.26	14.10
A2	6.26	14.10	5.50	16.05	5.50	16.05
C1	6.24	14.15	5.42	16.29	<5.28**	>16.72
C2	6.26	14.10	5.32	16.59	<5.28**	>16.72

* : Carbonate and organic matters removal.

** : broad peak

HIV ; A1 0.2-2 μ m XRD HIV
 . K 14 300
 EG . HIV . DCB
 14 DCB
 DCB A2, C1, C2 0.2-2 μ m EG
 DCB
 2:1 hydroxy-Fe/Mg/Al
 DCB HIS HIV K 14
 (Barnhisel and Bertsch, 1989). DCB
 XRD K 14 A1 A2-C2
 A2-C2 HIV HIS
 K HIV HIS (001) 10.1-10.5
 (Barnhisel, 1965). HIV HIS A1
 A2-C2
 HIV HIS EG 16.05-16.20
 . AIPEA , (0.6-0.9, half unit cell)
 (0.2-0.6, half unit cell) (Bailey, 1980).
 (Borchardt, 1989). 14 , 17
 가
 (Harward *et al.*, 1969; Robert, 1973, Malla *et al.*, 1987).
 가 ,
 가 Si⁴⁺가 Al³⁺
 (Robert, 1973).
 (Malla *et*

al., 1987). Al^{3+} Fe^{2+}
 Mg^{2+} 가 가
(16.05- 16.20) 가
가 가 가
가
A1, A2, C1, C2 HIV가 , K
A1 A2, C1, C2
. HIV 가 .
HIS ; Acid oxalate C1, C2 0.2-2 μm EG 17
C1
C2 가 . Acid oxalate
hydroxy-Al/Mg
C1 C2 acid oxalate
HIS가 .

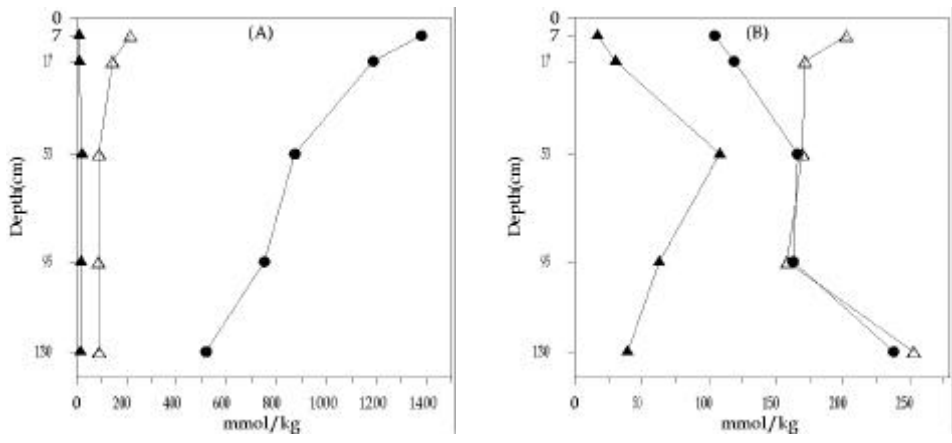


Fig. 15. Extractable Al, Fe, and Mg from clay size fractions with DCB, and acid oxalate. A: DCB treatment; B: acid oxalate treatment; open triangle: Al; solid triangle: Mg; solid circle: Fe.

HIV HIS ; HIV HIS
 hydroxy-Al/Mg/Fe , DCB acid oxalate
 Al, Fe, Mg HIV HIS
 (hydroxy-interlayered materials) . DCB
 hydroxy-Fe/Al/Mg , hydroxy-Fe
 (Ghabru, 1990). Acid oxalate hydroxy-Al/Mg
 (Rich, 1986; Wada and Kakuto, 1983; Matsue and Wada, 1988;
 Barnhisel and Berstch, 1989).

A1-C2 DCB acid oxalate . Acid oxalate
 hydroxy-Al/Mg 가 . Acid oxalate
 hydroxy-Al/Mg DCB , DCB
 hydroxy-Fe 가 . DCB Fe Al,
 Mg Fe가

(Fig. 15).

C1 C2 acid oxalate HIS
 . Acid oxalate Al A1 A2
 (Fig. 15). Mg A1 A2 16-30mmol/kg C1 C2
 62-108mmol/kg . hydroxy-Al
 , hydroxy-Mg (Rich, 1986).
 C1 C2 pH(H₂O) (7.25-7.37) C1 C2 hydroxy-Mg가
 가 .

5.2.

XRD , 가
 . <0.2 μ m /
 , 0.2-2 μ m / .

/ ; <0.2 μ m CR 0.2-2 μ m
 XRD . A1 Mg
 7.43 EG 7.62
 . K 7.5
 / (Wiewiora,
 1971; Hughes *et al.*, 1987).
 / EG
 001/002 002/005 ,
 (Cradwick and Wilson, 1972).
 / (peak decomposition)
 (Lanson, 1992).
 , / (Fig. 16).
 001/002 002/005 A1-CR
 (Table 12). 001/002 002/005
 (Cradwick and Wilson, 1972).
 (2) Moore Reynolds(1989)가
 84-86% (Fig. 17).
 /
 NEWMODE (Fig. 18). NEWMODE
 / , ,
 / 85%
 . XRD
 가 가 .
 / 80% 90% 가 ,
 14% 6% (Table 13).

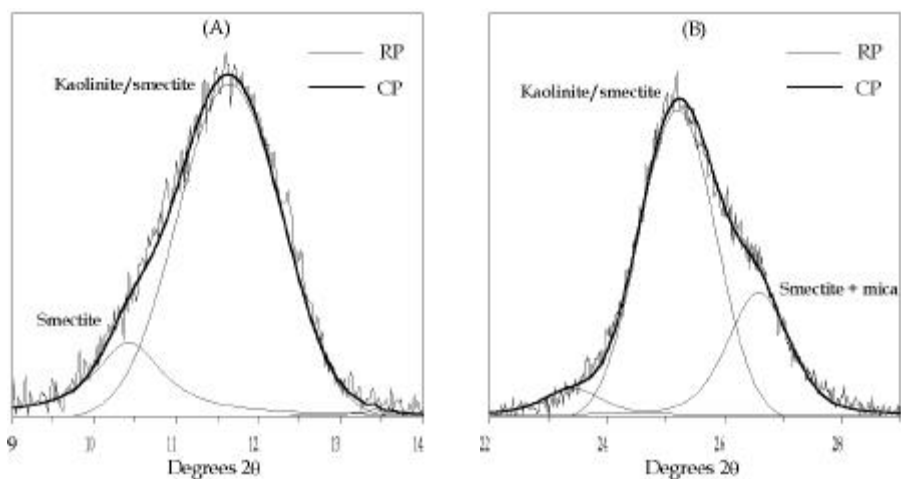


Fig. 16. Decomposition for XRD pattern of A1(<math><0.2\mu\text{m}</math>), after DCB, and EG treatment. RP: row pattern; CP: calculated pattern.; A: 001/002; B: 002/005 of kaolinite/smectite interstratification.

Table 12. The peak position of kaolinite/EG-smectite interstratification.

	size (μm)	001/002		002/005		2
		2	d ()	2	d ()	
A1	<math><0.2</math>	11.64	7.59	25.19	3.53	13.55
A2	<math><0.2</math>	11.62	7.60	25.12	3.54	13.50
C1	<math><0.2</math>	11.57	7.64	25.06	3.55	13.49
C2	<math><0.2</math>	11.61	7.61	25.16	3.53	13.55
CR	<math><0.2</math>	11.54	7.66	25.08	3.54	13.54
	2-0.2	11.57	7.64	25.09	3.54	13.52

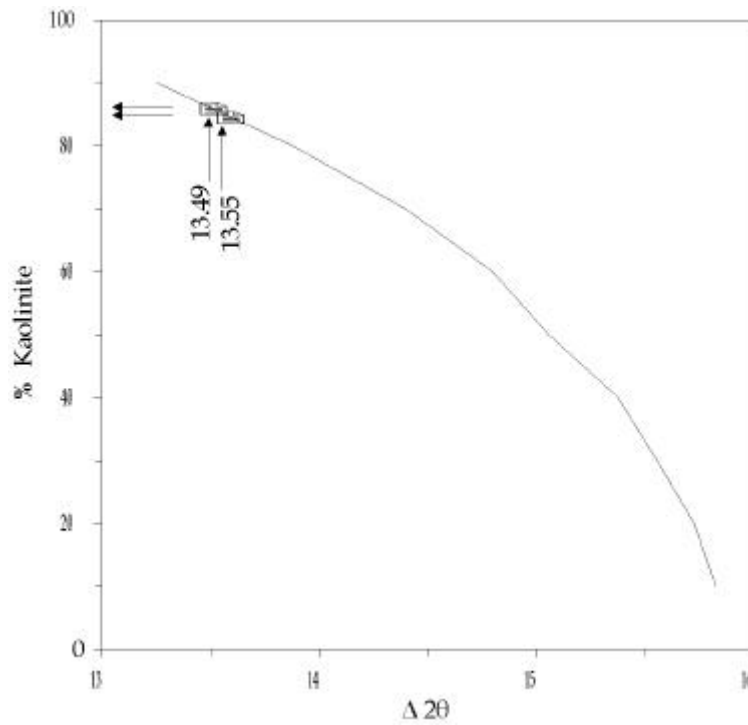


Fig. 17. The proportion of kaolinite in kaolinite/smectite interstratification.

Table 13. Mineral compositions of clay size fraction obtained by NEWMODE.

	size (μm)	%		
		Kaolinite/Smectite	Smectite	Mica
A1	<0.2	90	6	4
A2	<0.2	88	8	4
C1	<0.2	88	10	2
C2	<0.2	82	16	1
CR	<0.2	80	18	1
	0.2-2	80	14	4

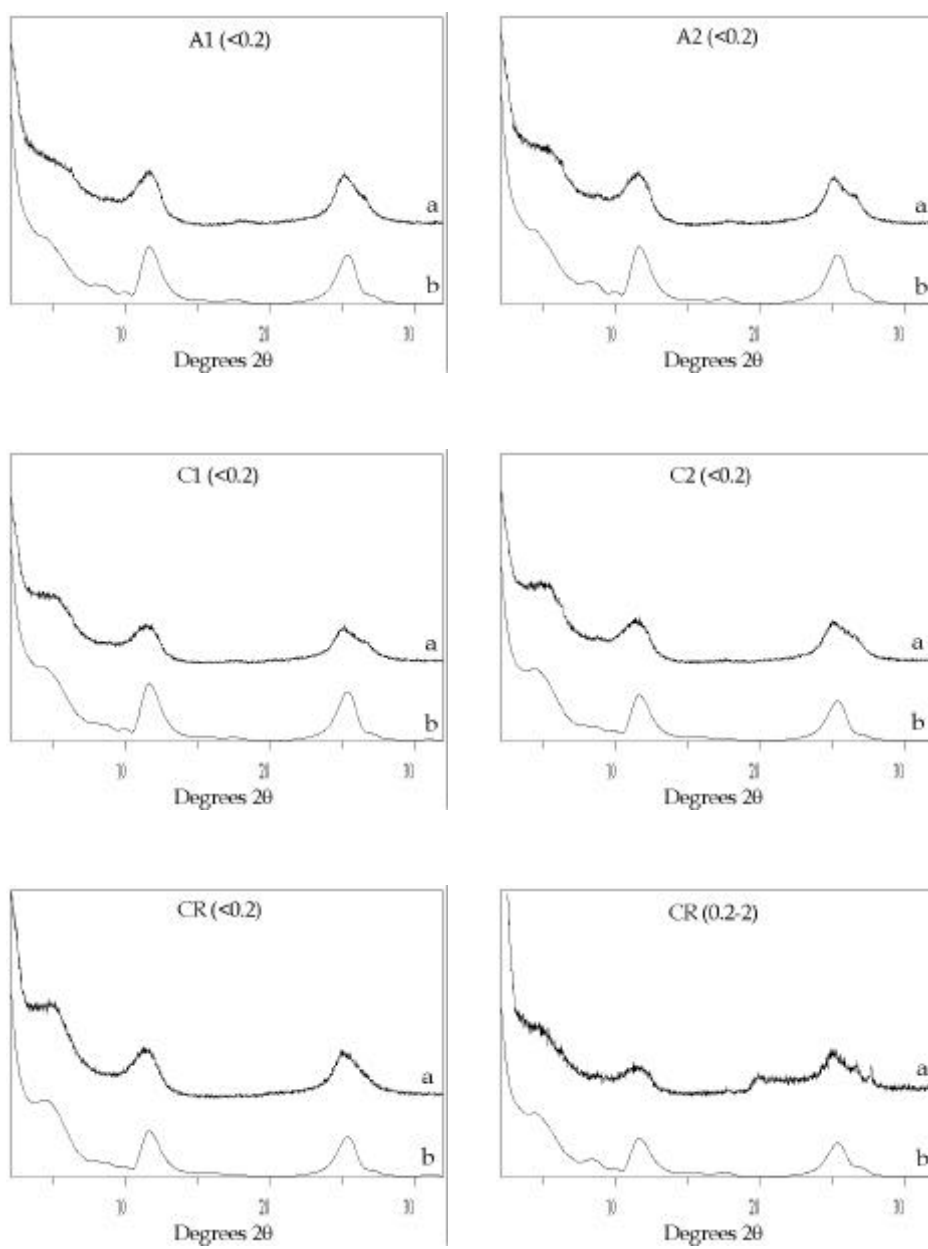


Fig. 18. Comparison of XRD patterns. a: EG treatment after DCB treatment; b: calculated with NEWMODE.

/ ; A1, A2, C1 0.2-2 μ m K
 12 8 가 . 110 , 300
 , 300 가 . 550 12
 가 가 . . EG 12
 , 7 가 .
 . 12 8
 (Brydon *et al.*, 1961). C2 EG .
 / /EG- 002/002,
 004/005 . 004/005
 , , 가
 002/002 . 002/002
 ,
 (peak decomposition) (Lanson, 1992).
 , / , 가
 (Fig. 19).

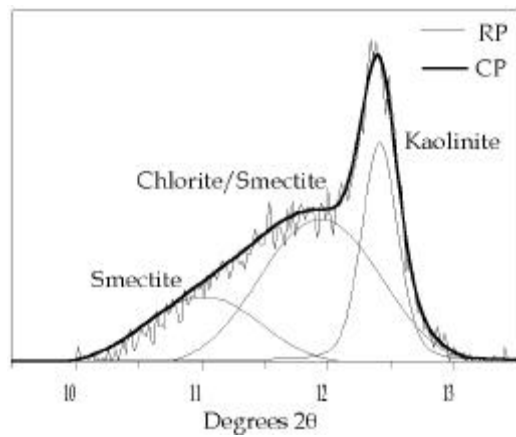


Fig. 19. Decomposition for XRD pattern of A1 (0.2-2 μ m), after DCB, and EG treatment.
 RP: row pattern; CP: calculated pattern.

/EG- 002/002 2 A1 11.94 A2, C1
 (Table 14). /
 R1 50% R0 (Moore and
 Reynolds, 1989). /
 002/002 Moore Reynolds(1989)가 /
 A1 70%
 C1 59% (Fig. 20). / 001/001
 002/002 , 550 가 가 .
 Fe (Brown and
 Brindley, 1980). /

NEWMODE

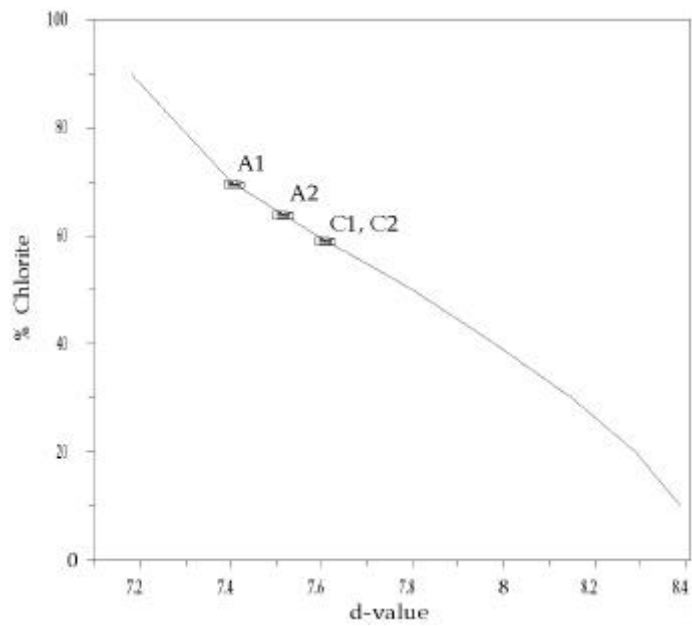


Fig. 20. The proportion of chlorite in chlorite/smectite interstratification.

Table 14. The peak position of chlorite/EG-smectite interstratification (0.2-2 μ m).

	002/002		% Chlorite
	2	d()	
A1	11.94	7.40	70
A2	11.77	7.51	64
C1	11.62	7.60	59
C2	11.62	7.60	59

5.3.

5.3.1.

Fig. 21

TiO₂

(Nesbitt, 1979).

$$variation(\%) = \frac{(element/TiO_2)_{sample} - (element/TiO_2)_{reference}}{(element/TiO_2)_{reference}} \times 100$$

CR . CR . Al₂O₃
 CR . Al₂O₃
 K₂O, Na₂O, CaO . Na⁺ Ca²⁺
 가 , Al³⁺ K⁺
 (Wada, 1986; Kurashima *et al.*, 1981).

가 . Si (leaching)
 가 .
 가 Si .

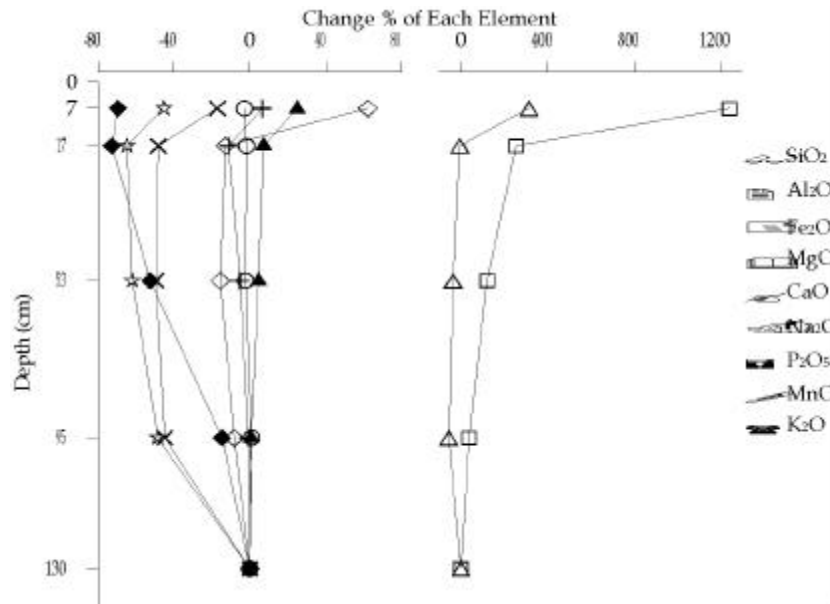


Fig. 21. The change of relative amounts of each elements to TiO₂.

(weathering index)

(K₂O, Na₂O, CaO, MgO) (Al₂O₃, Fe₂O₃, TiO₂)

(Coleman, 1982; Jenny, 1941).

(Parker, 1970).

Fig. 22

(molecular weight)

$$Base/R_2O_3 = \frac{K_2O + Na_2O + CaO + MgO}{Al_2O_3 + Fe_2O_3 + TiO_2}$$

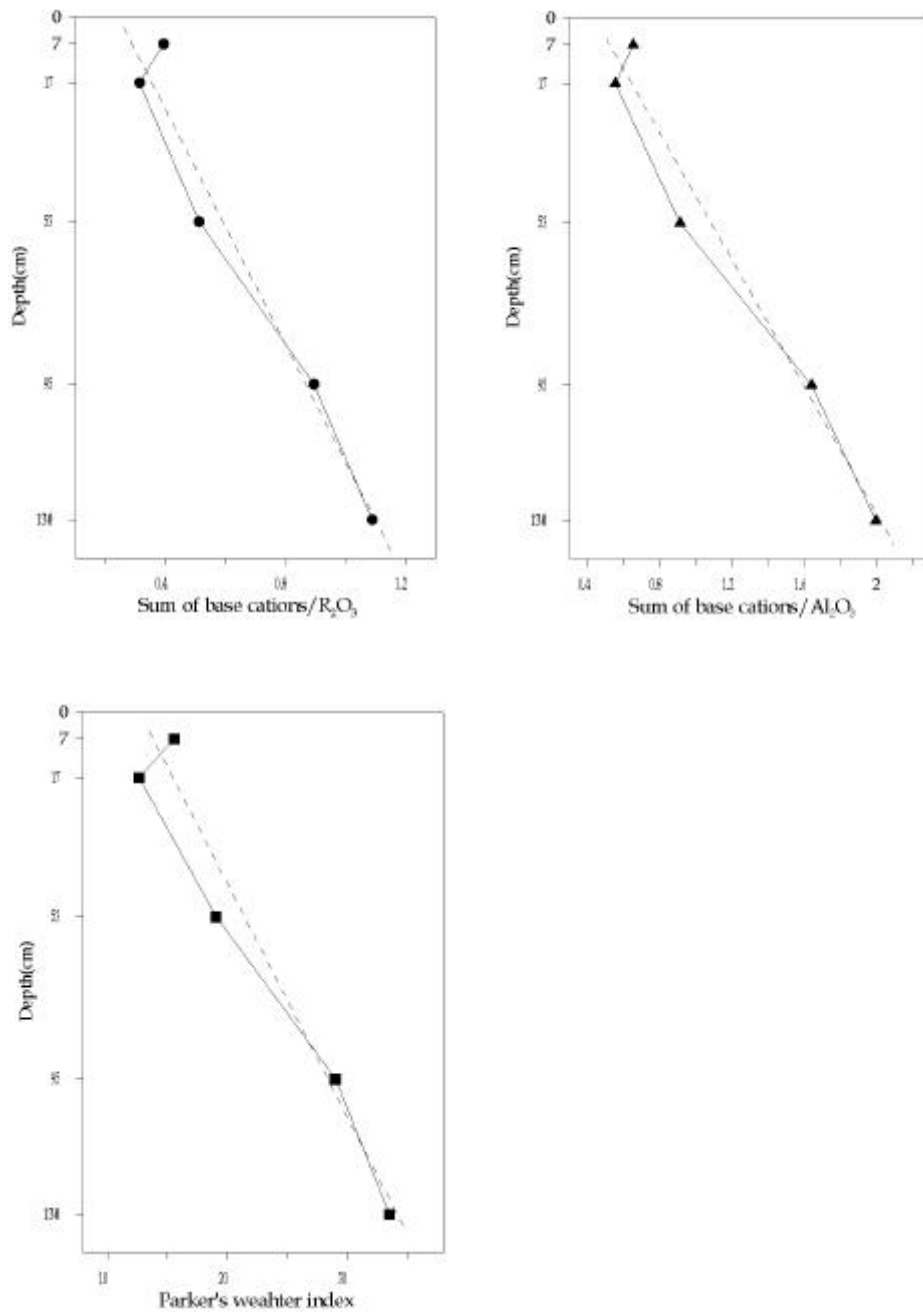


Fig. 22. Weathering indices of bulk samples.

$$Base/A\ llumina = \frac{K_2O + Na_2O + CaO + MgO}{Al_2O_3}$$

$$Parker's\ weathering\ index = \left(\frac{K_2O}{0.25} + \frac{Na_2O}{0.35} + \frac{CaO}{0.7} + \frac{MgO}{0.9} \right) \times 100$$

A1 A2 , A2 A1
 가 가 가
 가

(Fig. 23,24).

(La, Ce, Nd)가 (Dy, Yb)

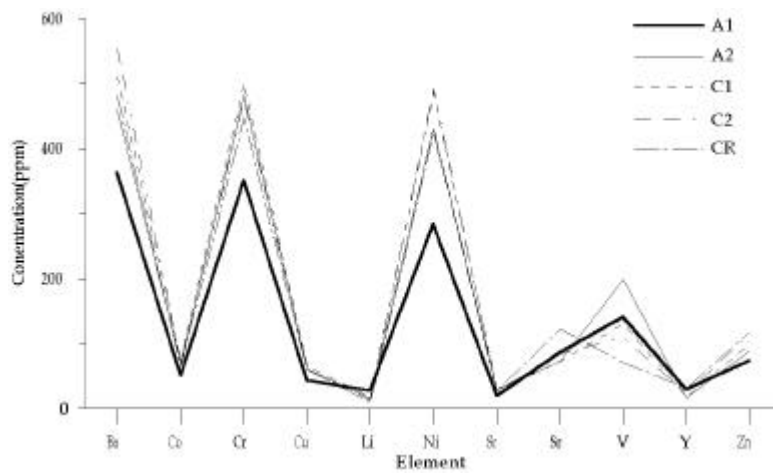


Fig. 23. Trace elements variation diagram for bulk.

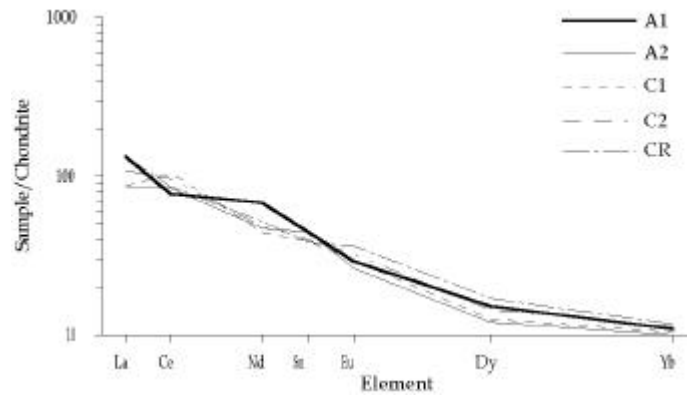


Fig. 24. Chondrite-normalized Rare Earth Element patterns for bulk.

5.3.2.

;

Andisols (Duchaufour, 1984; Shoji and Fujiwara, 1984; Saigusa and Shoji, 1986).

Andisols (Shoji *et al.*, 1993).

Andisols pH(H₂O),

Andisols pH(H₂O)

가

pH(H₂O) (<4.9)

2:1 Al/Fe- (Shoji *et*

*al.*1982; Shoji and Fujiwara, 1984). 가가 Si 가

Si (Parfitt, 1990).

pH(H₂O)가 가 (>4.9) allophane

가 Al/Fe- 가 Si

80% Andisols

(1.54-2.88wt%) (Song and Yoo, 1994; Shin and Tavernier, 1988).

가

1,872mm , 1,280mm

SiO₂ 37-49wt%

Andisols SiO₂ (22-30wt%) (Shin and Tavernier, 1988).

Si

; pH(NaF) 9.49-9.81

9.4 (Fieldes and Perrott, 1966).

(Parfitt and Childs,

1988). Acid oxalate Al(Al_o), Si(Si_o) Na-pyrophosphate

Al(Al_p) Al/Si (Childs *et*

al., 1983; Farmer *et al.*, 1983; Parfitt and Wilson, 1985). Al/Si

$$\frac{Al}{Si} = \frac{Al_o - Al_p}{Si_o}$$

Table 15. pH(NaF) and the amounts of short-range-order materials.

	pH (NaF)	Si _o mmol/kg	$\frac{Al_o - Al_p}{Si_o}$	Factor	SOM* wt%
A1	9.49	86	1.68	6.369	1.54
A2	9.63	114	0.92	4.844	1.95
C1	9.53	174	0.79	4.589	2.25
C2	9.55	210	0.69	4.370	2.57
CR	9.81	244	0.60	4.205	2.88

* : short-range-order materials

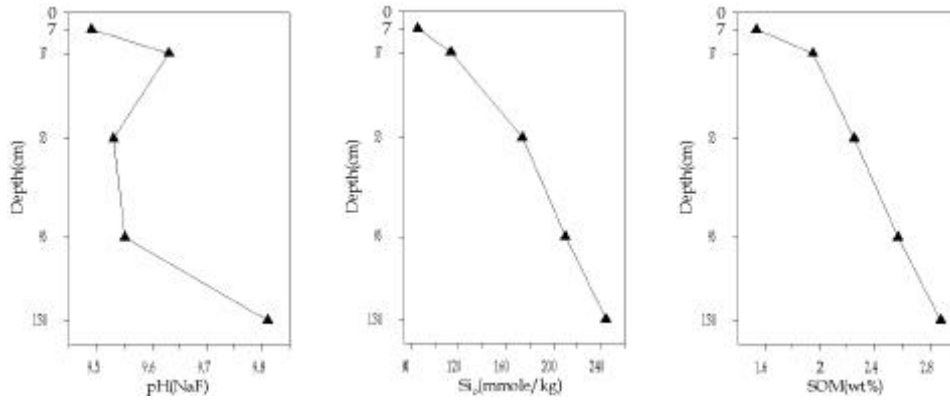


Fig. 25. pH(NaF), Si_o, and short-range-order materials of bulk samples.

acid oxalate

Al

Al/Si

1-2

(Parfitt, 1996).

Al_o - Al_p / Si_o 0.60- 1.68

1

(Table 15).

Al_o - Al_p / Si_o

(conversion factor)

(Parfitt, 1990),

Si_o

1.54- 2.88wt% . Si_o

가 가

가 (Fig. 25).

Si

;

가 가 . Si

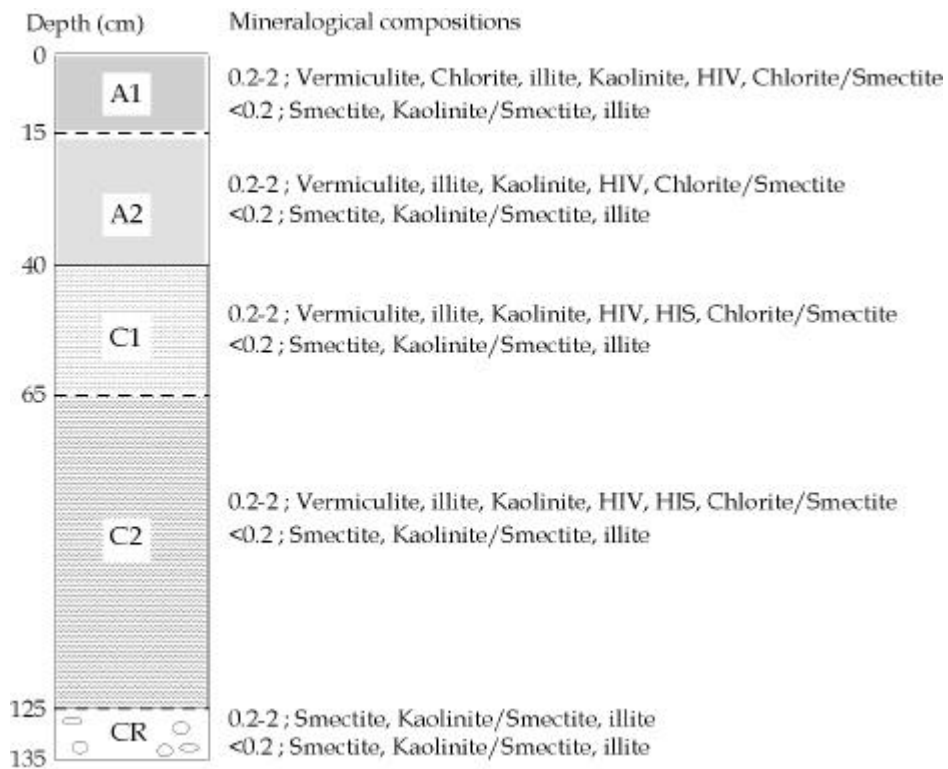
(Fig. 26).

0.2- 2μm

가 가

CR
 , HIV, HIS
 (Churchman, 1980; Ross and Kodama, 1974;
 Herbillon and Makumbi, 1975). 가
 가 HIV, HIS
 (Barnhisel and Berstch, 1989). Inoue(1981)
 가 HIV, HIS

Fig. 26. Variation of mineralogical compositions of clay size fractions with depth.



HIV가 .
HIV 가

hydroxy- (MacEwan and Wilson,
1980; Kittrick, 1983; Barnhisel and Berstch, 1989). HIV
 , hydroxy-Fe/Al . HIV hydroxy-Fe/Al
 가 가 , 가 가
 . / 가
 가 , 가 가

HIS가
 , 가 HIS가
 (Inoue, 1981). $<0.2\mu\text{m}$
 /

가 . pH(KCl)
 . pH(KCl) pH (pH-dependent charge)
 Al . pH
 . 7wt% 33wt% 가
 . pH(KCl) 5.1-5.3 가 . pH(KCl)
 가 pH(KCl)

가
 , HIV HIS,
 가

;

(, 1998).

, 가

가

가

(Mizota and Inoue, 1988; Inoue and Narse, 1991).

가

(Eswaran, 1972).

A

CR

CR

C

가

C

가

A

가

가

6

,
 .
 , , .
 , .
 , 0.8-2wt% , pH(H₂O) 6.6-7.3
 Andisols pH(H₂O) <6.0 . pH(NaF)
 9.49-9.81 , 1.54-2.88(wt%) 가
 가 .
 , 0.2-2 μ m , , , , ,
 . / ,
 hydroxy-Al/Mg/Fe . C
 HIS HIV가 , A HIV . HIV
 DCB hydroxy-Fe/Al .
 HIS acid oxalate hydroxy-Mg/Al ,
 hydroxy-Mg가 . /
 59-70% 가 가 .
 , <0.2 μ m / ,
 , . / ,
 84-86% . 가
 , / 가 .
 가
 , HIS, , HIV
 .

- , , , (1989) ().
- KR-88-(B)-4, p. 1-49.
- (1976) .
- (1996) . p. 145-290.
- (1976) . v. 12, p. 207-226.
- (1999) . p, 34-44.
- (1993) .
- (1998) . v. 7, p. 1-14.
- Bailey, S.W. (1980) Summary of recommendation of AIPEA Nomenclature Committee. *Clay Miner.* v. 15, p. 85-93.
- Barnhisel, R.I. (1965) The formation and stability of aluminum interlayers in clays. Ph.D. diss., Virginia Polytechnic Inst., Blacksburge. *Diss. Abstr.* p. 65-5066.
- Barnhisel, R.I. and Berstch, P.M. (1989) Chlorites and Hydroxy interlayered vermiculite and smectite. p. 729-788. *In* J.B. Dixon and S.B. Weed(ed.) *Minerals in soil environment.* SSSA. Mdison, WI.
- Bautista-Tulin, A.T. and Inoue, K. (1997) Hydroxy-interlayered minerals in Japanese soils influenced by eolian deposition. *Soil Sci. Soc. Am. J.* v. 61, p. 631-640.
- Brindley, G.W. (1966) Ethylene glycol and glycerol complexes of smectites and vermiculites. *Clay Miner. Bull.* v. 6, p. 237-259.
- Brown, G.E. and Brindley, G.W. (1980) X-ray diffraction procedures for clay mineral identification. v. 5, p. 305-359. *In* Brindley, G.W. and Brown, G.E.(ed.) *Crustal structures of clay minerals and their X-ray identification.*

- Mineral. Soc., London.
- Brydon, J.E., Clark, J.S. and Osborn, v. (1961) Dioctahedral chlorite. *Can. Mineral.* v. 6, p. 595-609.
- Childs, C.W., Parfitt, R.L. and Lee, R. (1983) Movement of aluminum as an inorganic complex in some podzolised soils, New Zealand. *Geoderma* v. 29, p. 39-155.
- Churchman, G.J. (1980) Clay minerals formed micas and chlorites in some New Zealand soils. *Clay Miner.* v. 15, p. 59-76.
- Colman, S.M. (1982) Chemical weathering of basalts and andesites: Evidence from weathering rinds. U.S. Geol. Surv. Prof. Pap.
- Cradwick, P.D., and Wilson, M.J. (1972) Calculated x-ray diffraction profiles for interstratified kaolinite-montmorillonite. *Clay Miner.* v. 9, p. 395-405.
- Duchaufour, P. (1984) *Pedologie*, Masson, Paris.
- Eswaran, H. (1972) Morphology of allophane, imogolite and halloysite. *Clay Miner.* v. 9, p. 281-285.
- Famer, V.C., Russell, J.D. and Smith, B.F.L. (1983) Extraction of inorganic forms of translocated Al, Fe and Si in a podzol Bs horizon. *J. Soil Sci.* v. 34, p. 571-576.
- Fieldes, M., and Perrott, K.W. (1966) The nature of allophane in soils. . Rapid field and laboratory test for allophane. *N.Z. J. Sci.*, v. 9, p. 623-629.
- Gee, G.W. and Bauder, J.W. (1986) Particle-size Analysis. p. 383-411. *In* Methods of soil analysis: Part 1 - Physical and mineralogical methods. 2nd edition. SSSA Book series. Madison, Wisconsin USA.
- Ghabru, S.K., mermut, A.R. and Arnaud, R.J. (1990) Isolation and characterization of an Iron-rich chlorite-like mineral from soil clays. *Soil Sci. Soc. Am. J.*, v. 54, p. 281-287.
- Harward, M.E., Carstea, D.D. and Sayegh, A.H. (1969) Properties of vermiculites and smectites: expansion and collapse. *Clays Clay Miner.* v. 16,

p. 437-447.

- Herbillion, A.J. and Makumbi, M.H. (1975) Weathering chlorite in a soil derived from a chlorite-schist under humid tropic conditions. *Geoderma*, v. 13, p. 89-104.
- Hughes, R.E., DeMaris, P.J., White, W.A. and Cowin, D.K. (1987) Origin of clay minerals in Pennsylvanian strata of the Illinois Basin. *In* Schultz, L.G., van Olphen, H., and Mumpton, F.A.(ed). *Internatl. Clay Conf.*, Denver, 1985, The clay minerals Society, Bloomington, Ind., p. 97-104.
- Inoue, K. (1981) Implication of eolian dusts to 14 minerals in the volcanic ash soils in Japan. *Pedologist* v. 25, p. 97-118.
- Inoue, K. and Naruse, T. (1991) Accumulation of Asian long-range eolian dust in Japan and Korea from the late Pleistocene to the Holocene. p. 25-42. *In* S. Okuda et al. (ed.) *LOESS Geomorphological hazards and processes*. Catena Suppl. 20. Catena Verlag, Cremlingen, Germany.
- Jackson, M.L. (1985) *Soil chemical analysis-Advanced course*. 2nd edition. 11th printing. Published by the author, Madison, Wisconsin. 53705, p. 100-113.
- Jenny, H. (1941) *Factors of soil formation*. McGraw-Hill, New York.
- Kim, D.H., Hwang, J.H., Hwang, S.L., Howells, M.F. and Reedman, A.J. (1986) Tuff rings and cones on Jeju Island, Korea. *J. Geol. Soc. Korea*, v. 22, p. 1-9.
- Kittrick, J.A. (1983) Chlorites differentiated from intergrade smectites and vermiculites by solution stability criteria. *Clays Clay Miner.* v. 31, p. 317-318.
- Lanson, B and Besson, G. (1992) Characterization of the end of smectite-to-illite transformation: Decomposition of X-ray patterns. *Clays and Clay Minerals*. v. 40. p. 40-52.
- Kurashima, K. Shoji, S. and Yamada, I. (1981) Mobilities and related factors of chemical elements in the top soils of Andisols in Tohoku, Japan: 1.

- Mobility sequence of major chemical elements. *Soil Sci.* v. 132, p. 300-307.
- Lee, M.W. (1982) Petrology and geochemistry of Jeju volcanic island, Korea. *Sci. Rpt. Tohoku Univ.*, v. 3, p. 177-256.
- Lee, S.K., Cha, K.S. and Kim, I.T. (1983) Studies on the physico-chemical properties and characterization of soil organic matter in Jeju Volcanic Ash Soil. *J. Korean Soc. Soil Sci. Fert.* v. 16.
- MacEwan, D.M.C. and Wilson, M.J. (1980) Interlayers and intercalation complexes of clay minerals. p. 197-248. *In* Brindley, G.W. and Brown, G.(ed). *Crystal structures of clay minerals*. Mineralogical Society, London.
- Malla, P.B. and Douglas, L.A. (1987a) Layer charge properties of smectite and vermiculites: Tetrahedral vs. Octahedral. *Soil Sci. Soc. Am. J.* v. 51, p. 1362-1366.
- Mausue, N. and Wada, K. (1988) Interlayer materials of partially interlayered vermiculite in Dystrichrepts derived from Tertiary sediments. *J. Soil Sci.* v. 39, p. 155-162.
- McKeague, J.A. and Day, J.H. (1966) Dithionite- and oxalate-extractable Fe and Al as aids in differentiation various classes of soils: *Can. J. Soil Sci.* v. 46, p. 13-22.
- Mizota, C. (1982) Tropospheric origin of quartz in Ando soils and Red-Yellow soils on basalts. *Japan. Soil Sci. Plant Nutr.* v. 28, p. 517-522.
- Mizota, C. and Inoue, K. (1988) Eolian dust contribution to soil development on volcanic ashes in Japan. p. 547-557. *In* D.I. Kinloch *et al.* (ed.) *Proc. Int. Soil Classif. 9th, Japan. 20 July-1 Aug. 1987. Soil Manage. Support Serv.*, Washington, DC.
- Moore, D.M. and Reynolds, R.C. (1989) X-ray diffraction and the identification and analysis of clay minerals. Oxford University Press, Oxford and New York.
- Nakamura, E., Campbell, I.H., McCulloch, M.T. and Sun, S.S. (1989) Chemical

- geodynamics in a back arc region around the Sea of Japan: Implications for the genesis of alkaline basalts in Japan, Korea and China. *J. Geophys. Res.*, v. 94, p. 4634-4654.
- Nesbitt, H.W. (1979) Mobility and fractionation of rare earth elements during weathering of a granodiorite. *Nature*, v. 279, p. 206-210.
- Parfitt, R.L. (1990) Allophane in new Zealand - a review. *Aust. J. Soil Res.* v. 28, p. 343-360.
- Parfitt, R.L. and Chlids, C.W. (1988) Estimation of forms of Fe and Al: A review, and analysis of contrasting soils by dissolution and Moessbauer methods. *Aust. J. Soil Res.*, v. 26, p. 121-144.
- Parfitt, R.L. and Wilson, A.D. (1985) Estimation of allophane and halloysite in three sequences of volcanic soils, New Zealand. *Catena Suppl.*, v. 7, p. 1-8.
- Parker, A (1970) An index of weathering for silicate rocks. *Geol. Mag.*, v. 107, p. 501-502.
- Rich, C.I. (1968) Hydroxy interlayers in expansible layer silicate. *Clays Clay Miner.* v. 16, p. 15-30.
- Robert, M. (1973) The experimental transformation of mica toward smectite. Relative importance of total charge and tetrahedral substitution. *Clays Clay Miner.* v. 21, p. 167-174.
- Ross, G.J. and Kodama, H. (1974) Experimental transformation of a chlorite into a vermiculite. *Nature(London)*, v. 255, p. 133-134.
- Saigusa, M. and Shoji, S. (1986) Surface weathering in Zao tephra dominated by mafic glass. *Soil Sci. Plant Nutr.*, v. 32, p. 617-628.
- Shin, J.S. and Travernier, R. (1988) Composition and genesis of volcanic ash soils in Jeju Island. . *Mineralogy of sand, silt and clay fractions. J. Miner. Soc. Korea*, v. 1, p. 40-47.
- Shoji, S., Dahlgren, R. and Nanzyo, M (1993) Genesis of volcanic ash soils. p.

- 37-71. *In* Shoji et al. (ed.) Volcanic ash soils; Genesis, properties and utilization. Developments in Soil Sci. 21, Elsevier.
- Shoji, S and Fujiwara, T. (1984) Active aluminum and iron in the humus horizons of Andosols from northeastern Japan: Their forms, properties, and significance in clay weathering. *Soil Sci.*, v. 137, p. 216-226.
- Shoji, S., Fujiwara, Y., Yamada, I. and Saigusa, M. (1982) Chemistry and clay mineralogy of Ando soils, Brown forest soils, and Podzolic soils formed from recent Towada ashes, northeastern Japan. *Soil Sci.*, v. 133, p. 69-86.
- Soil Survey Staff (1992) Soil survey laboratory methods manual. Soil Survey Investigation Rep. 42. USDA-NRCS. U.S. Gov. Print. Office, Washington, DC.
- Soil Survey Staff (1996) Soil survey laboratory methods manual. Soil Survey Investigation Rep. 42. USDA-NRCS. U.S. Gov. Print. Office, Washington, DC.
- Song, K.C. and Yoo, S.H. (1994) Andic properties of major soils in Cheju Island . Condition for Formation of Allophane. *J. Korean Soc. Soil Sci. Fert.* v. 27, p. 149-157.
- Suquet, H., de la Calle, C., Pezerat, H. (1975) Swelling and structural organization of saponite. *Clays Clay Miner.* v. 23, p. 1-9.
- Taylor, S.R. and McLennan, S.M. (1985) The continental crust: It's composition and evolution. Blackwell, Oxford.
- Wada, K. and Kakuto, Y. (1983) Intergradient vermiculite-kaolinite mineral in Korean Ultisols. *Clays Clay Miner.* v. 31, p. 183-190.
- Wada, K. (1986) Part . Database, Kurobokudo Co-operative Research Group. p. 115-276. *In* K, Wada (ed.) Ando soils in Japan. Kyushu University Press, Fukuka, Japan.
- Walsh, J.N. (1980) The simultaneous determination of the major, minor and trace constituents of silicates rocks using inductively coupled plasma

- spectrometry. *Spectrochim. Acta*, v. 35B, p. 107- 111.
- Wiewiora, A. (1971) A mixed-layer kaolinite-smectite from Lower Silesia, Poland: *Clays and Clay minerals*. v. 19, p. 415-416.
- Yoo, S.H. and Song, K.C. (1984) Chemical characteristics of soils in Cheju Island . Variations in chemical characteristics with altitude. *J. Korean Soc. Soil Sci. Fert.* v. 17.
- Zhang, Y.F., Inoue, K. and Sase, T. (1994) A long-range transported eolian dust found in tephra of the Iwata Volcano after the fall of the Toya Ash. *Quat. Res.* v. 33, p. 131- 151.

Abstract

Mineralogical Transformation of a Soil derived from Volcanic Sediments, Dangsangebong, Jeju Island

Ha, dae-ho

Dept. of Earth System Sciences

The Graduate School

Yonsei University

About 80% of Jeju soils derived from volcanic ash are classified as Andisols, while the soils derived from Dangsangebong is not Andisols. There is a significant difference in distribution of precipitation in Jeju island. The study area is characterized by the lowest amount of annual rainfall in Jeju Island, and the layered silicates as dominant solid phase in clay fraction of the volcanogenic soils. The purpose of this study is to characterize the layer silicates and to clarify the formation and weathering sequences of Dangsangebong soils.

Two master soil horizons are recognized in the soil profile developed in the Dangsangebong area, which can be designated as A and C. The soil pH(H₂O), ranges from 6.6 to 7.3 increasing with depth, is higher than that of typical Andisols. While the pH(NaF), ranges from 9.49 to 9.81, indicates that significant amount of amorphous phases might be present as exchanging complexes. It is estimated to about 1.54-2.88wt% by using chemical selective dissolution. The organic content of surface horizon is about 2wt%. This soil are composed of quartz, feldspar and olivine as major constituents with minor

of silicate clays. Quartz is frequently observed in A and distinctly decreases in its amount with depth, where olivine is dominant phase in C, and is rarely observed in A.

In the $<0.2\mu\text{m}$ size fraction, smectite and kaolinite/smectite interstratification are dominant with minor of illite. The amounts of smectite decrease with depth, while the amounts of kaolinite/smectite interstratification increase with depth, which indicates the trend of mineral transformation with increasing the degree of weathering. The proportion of kaolinite in kaolinite/smectite interstratification is about 85%, and is not changed severely through the profile.

In the $2-0.2\mu\text{m}$ size fraction, vermiculite, smectite, illite and kaolinite are major components with minor of chlorite. Most of chlorite are interstratified with smectite. Chlorite which is not interstratified with smectite occurs only in surface horizon. The proportion of the chlorite in the chlorite/smectite interstratification is 59-70% and increases with depth. Hydroxy-interlayered vermiculite(HIV) with hydroxy-Fe/Al in their interlayers occurs in both A and C horizon. The amounts of hydroxy-Fe/Al decrease with depth. Hydroxy-interlayered smectite(HIS) of which interlayers might be composed of hydroxy-Mg/Al occurs only in C horizon.

As the results of mineralogical investigation for the soil profile in the study area, clay minerals might be changed and evolved through the following weathering sequence; 1) Smectite Kaolinite, HIS, Vermiculite, 2) Vermiculite HIV Chlorite.

Key words :

Dangsanbong, volcanic ash, layered silicates, HIV, HIS, chlorite/smectite, kaolinite/smectite, weathering sequence.